

**USE ATYPICAL ASPHALT BINDERS FROM ALBERTA  
OILSAND SOURCES FOR THE EFFECTIVE RECYCLING  
OF ASPHALT PAVEMENT**

by

**CHANAKA NAWARATHNA**

A thesis submitted to the Department of Chemistry  
in conformity with the requirements for the  
Degree of Master of Science

Queen's University

Kingston, Ontario, Canada

(March, 2021)

Copyright © Chanaka Nawarathna, 2021

## ***Abstract***

Utilization of Reclaimed Asphalt Pavement (RAP) and Reclaimed Asphalt Shingles (RAS) optimizes the use of natural resources by saving the cost for virgin asphalt binders and therefore reducing their environmental footprint. This thesis presents experimental results of using RAP and RAS with virgin asphalt binders from Alberta oil sands deposits.

Virgin asphalt binder A from the Athabasca deposit and virgin asphalt binder C from the Cold Lake deposit were modified at two different RAP weight percentages (20 % and 40 % by weight of the total binder). Each blend was tested under four different aging conditions (Unaged, Rolling Thin Film Oven-aged (RTFO), Pressure Aging Vessel-aged (PAV) for 20 h (PAV-20) and 40 h (PAV-40)). The RAP sources used in this study came from rehabilitation contracts on Highway 7 and Highway 403, while tear-off shingles were used as a source of RAS binder. Fourier Transform Infrared (FTIR) spectrometry was used to monitor the degree of oxidation when binders were modified with RAP and RAS and subsequently aged in RTFO and PAV. Rheological properties of the modified binders after different aging protocols were assessed using a Dynamic Shear Rheometer (DSR). Hot Mixed Asphalt (HMA) tests were conducted for neat asphalt binders, 20 % RAP-modified binders and Polyethylene Terephthalate (PET)-modified binders using the Illinois Flexibility Index Test (I-FIT) at two different temperatures (room temperature and -10 °C).

Rheological results showed that virgin binder A is the softer one and therefore accommodates more RAP than C. The results also reveal that 20 % RAP added to A can be used as a lower cost alternative for virgin C, as the two materials possess nearly the same rheological grade. According to the I-FIT results, using neat A with 20 % RAP gives higher flexibility than using neat C for HMA. Finally, using PET fibers with virgin binders drastically increases the flexibility of the HMA in the semi-circular bending test.

## *Acknowledgment*

First and foremost, I take the immense pleasure of thanking my supervisor, Prof. Simon A. M. Hesp for the tremendous support throughout my research project with his knowledge, motivation and patience. Without his persistent help, the goal of this project would not have been realized. Next, I wish to show my gratitude to my supervisory committee, Prof. Donal Macartney and Prof. Guojun Liu for their valuable suggestions and feedback on the success of this project.

My appreciation goes to Alberta Innovates and all other material suppliers for their contribution throughout the Master program. I would like to pay my special regards to Ahmed Khan, Emmanuella Asiedu, Justice Gyasi and Haibo Ding for guiding and assisting me in carrying out lab experiments. I extend my gratitude to my colleagues, Abiola Adeyeye, Emil Khusainov and Oluwatobi Oyebanji for their support in various ways to the successful completion of this thesis. I am indebted to the Department of Chemistry at Queen's University for the opportunity and for providing me with the necessary resources and other technical support.

I express my deepest gratitude to my parents, Mr. H.M Nawarathna and K.M Kulasekara, my wife, Mrs. Thakshila Dharmasena and my sister, Bhagya Nawarathna for their support and encouragement throughout my carrier. Finally, I would like to thank all my teachers for their guidance and for giving me knowledge.

# **Content**

<i>Abstract</i> .....	<i>ii</i>
<i>Acknowledgement</i> .....	<i>iii</i>
<i>List of figures</i> .....	<i>vii</i>
<i>List of tables</i> .....	<i>x</i>
<i>List of abbreviations</i> .....	<i>xi</i>
<i>Chapter 1- Introduction</i> .....	<i>1</i>
<i>1.1 Overview</i> .....	<i>1</i>
<i>1.2 Asphalt cement and applications</i> .....	<i>3</i>
<i>1.3 Chemical composition of Asphalt</i> .....	<i>4</i>
<i>1.4 Source of asphalt</i> .....	<i>6</i>
<i>1.5 Asphalt Specifications</i> .....	<i>7</i>
<i>Chapter 2- Literature review</i> .....	<i>10</i>
<i>2.1 Aging of Asphalt</i> .....	<i>10</i>
<i>2.2 Simulate asphalt aging in laboratory conditions</i> .....	<i>11</i>
<i>2.2.1 Rolling Thin-Film Oven</i> .....	<i>11</i>
<i>2.2.2 Pressure Aging Vessel (PAV)</i> .....	<i>12</i>
<i>2.3 Failures of asphalt pavements</i> .....	<i>13</i>
<i>2.3.1 Permanent deformation (Rutting)</i> .....	<i>13</i>
<i>2.3.2 Fatigue cracking</i> .....	<i>14</i>
<i>2.3.3 Thermal cracking / low temperature cracking</i> .....	<i>16</i>
<i>2.3.4 Moisture damage</i> .....	<i>17</i>
<i>2.4 Conventional testing methods for Asphalt binders</i> .....	<i>18</i>
<i>2.4.1 Penetration test</i> .....	<i>18</i>
<i>2.4.2 Ring and Ball Softening Point Test</i> .....	<i>20</i>

2.4.3 Viscosity Test.....	21
2.5 Superpave Testing Methods.....	22
2.5.1 Fourier Transform Infrared (FTIR) Spectroscopy.....	23
2.5.2 Dynamic Shear Rheometer (DSR).....	25
2.5.3 Bending Beam Rheometer.....	28
2.6 Ministry of Transportation of Ontario (MTO) Methods.....	30
2.6.1 Extended Bending Beam Rheometer (EBBR).....	31
2.6.2 Double Edge Notched Tension (DENT) Test.....	31
2.7 Hot mixed asphalt (HMA) testing.....	33
2.7.1 Superpave gyratory compactor (SGC).....	33
2.7.2 Illinois Flexibility Index Test (I-FIT).....	34
2.8 Modifications of asphalt.....	36
2.8.1 Polyethylene terephthalate (PET) as a modifier.....	37
2.8.2 Reclaimed Asphalt materials as asphalt modifiers.....	38
2.9 Chemical compatibility of modifications.....	39
Chapter 3- Materials and Experimental Methods.....	41
3.1 Materials.....	41
3.2 Recovery of reclaimed asphalt.....	41
3.3 Modification of neat asphalt binders.....	42
3.4 Aging of asphalt binder.....	42
3.4.1 Short term aging.....	42
3.4.2 Long term aging.....	43
3.5 Dynamic Shear Rheometer.....	43
3.6 Fourier Transform Infrared (FTIR) Spectroscopy.....	44
3.7 Hot Mixed Asphalt (HMA).....	45

3.7.1	<i>Preparation of test specimens</i> .....	46
3.7.2	<i>Illinois Flexibility Index Test (I-FIT)</i> .....	47
Chapter 4-	<i>Results and Discussion</i> .....	49
4.1	<i>Dynamic Shear Rheometer tests results</i> .....	49
4.1.1	<i>High Temperature Performance Grade (HTPG)</i> .....	49
4.1.2	<i>Limiting phase angle temperatures</i> .....	52
4.1.3	<i>Grade span</i> .....	59
4.1.4	<i>High Temperature Performance Grade with limiting phase angle</i> ...	62
4.1.5	<i>Black space diagram</i> .....	63
4.2	<i>FT-IR data analysis</i> .....	64
4.3	<i>Hot Mixed Asphalt test results</i> .....	65
4.3.1	<i>Force-Displacement curves</i> .....	66
4.3.2	<i>Normalized Fracture Energy (Gf)</i> .....	67
4.3.3	<i>Flexibility Index (FI)</i> .....	69
Chapter 5-	<i>Summery</i> .....	72
References	.....	74

## ***List of Figures***

<b>1.1</b>	Schematic of (SARA) chromatographic method .....	5
<b>1.2</b>	Location of the heavy-oil/bitumen deposits in America .....	6
<b>1.3</b>	Locations of the three main oil sands deposits in Northern Alberta .....	7
<b>2.1</b>	Rolling Thin-Film Oven .....	12
<b>2.2</b>	Pressure Aging Vessel .....	12
<b>2.3</b>	Rutting on asphalt pavement .....	14
<b>2.4</b>	Fatigue cracking .....	15
<b>2.5</b>	Low temperature cracking .....	17
<b>2.6</b>	Moisture damage .....	18
<b>2.7</b>	Penetration test .....	20
<b>2.8</b>	Ring and Ball Apparatus .....	21
<b>2.9</b>	Brookfield viscometer and vacuum capillary viscometer .....	22
<b>2.10</b>	FTIR spectrometer and sample FTIR spectrum for asphalt .....	24
<b>2.11</b>	Stress-strain response during oscillatory testing. a) Purely elastic response, b) purely viscous response and c) viscoelastic response .....	26
<b>2.12</b>	Representation of phase angle ( $\delta$ ). a) $\delta$ as an indicator of the relative amounts of recoverable ( $G'$ ) and non-recoverable ( $G''$ ) deformation and b) $\delta$ as the phase difference between stress and strain in harmonic oscillation .....	26
<b>2.13</b>	Representation of parallel plate configuration of DSR plates .....	27
<b>2.14</b>	Schematic representation of DSR operation .....	27
<b>2.15</b>	DSR Instrument .....	28
<b>2.16</b>	Deflection measured against time in the BBR test .....	29
<b>2.17</b>	Bending Beam Rheometer .....	30
<b>2.18</b>	Double-Edge-Notched Tension (DENT) design .....	33

<b>2.19</b> Superpave Gyrotory compactor (SGC) .....	34
<b>2.20</b> Force-displacement curve in I-FIT .....	35
<b>2.21</b> a) SCB test specimen and configuration and b) geometry of specimen.....	35
<b>2.22</b> Molecular Structure of Polyethylene Terephthalate (PET) .....	37
<b>3.1</b> RTFO aging. a) Loading the glass tube, b) Rolling in RTFO and c) coated tube after aging.....	43
<b>3.2</b> Pine Instruments gyrotory compactor .....	46
<b>3.3</b> Cutting the specimen a) in to halves, b) notch along the axis .....	47
<b>3.4</b> Illinois Flexibility Index Test .....	48
<b>4.1</b> Changes of HTPG with adding RAP and RAS into base asphalts. a) HTPG of C asphalt blends, b) HTPG of A asphalt blends and c) Comparison of HTPGs of C based asphalt blends and A based asphalt blends.....	50
<b>4.2</b> Limiting phase angle temperatures of two base asphalts at unaged and PAV-20 hours aging conditions, a) $T_{\delta=30^{\circ}}$ and b) $T_{\delta=45^{\circ}}$ .....	53
<b>4.3</b> $T_{\delta=30^{\circ}}$ of asphalt blends at unaged and PAV-20 hours aging conditions, a) C based asphalt blends and b) A based asphalt blends .....	54
<b>4.4</b> $T_{\delta=45^{\circ}}$ of asphalt blends at unaged and PAV-20 hours aging conditions, a) C based asphalt blends and b) A based asphalt blends .....	55
<b>4.5</b> $T_{\delta=45^{\circ}}$ comparison with base C binder (Unaged condition). a) 20% RAP and RAS with base C and b) 20% RAP and RAS with base A.....	57
<b>4.6</b> $T_{\delta=45^{\circ}}$ comparison with base C binder (PAV-20 hours aging condition). a) 20% RAP and RAS with base C and b) 20% RAP and RAS with base A.....	58
<b>4.7</b> $T_{\delta=30^{\circ}}$ comparison with base C binder (Unaged condition). a) 20% RAP and RAS with base C and b) 20% RAP and RAS with base A.....	58

<b>4.8</b> $T_{\delta=30^\circ}$ comparison with base C binder (PAV-20 hours aging condition). a) 20% RAP and RAS with base C and b) 20% RAP and RAS with base A.....	59
<b>4.9</b> Grade span of two neat asphalts a) Unaged conditions b) PAV-20 hours aging condition.....	59
<b>4.10</b> Grade spans for asphalt binder blends included C and A base asphalts (a) unaged samples (b) PAV-20 hours aged samples.....	60
<b>4.11</b> Grade span comparison of base C with A + RAP blends a) Unaged b) PAV-20 hours aged samples .....	61
<b>4.12</b> Grade span comparison of base C with A + RAP blends a) Unaged b) PAV-20 hours aged samples .....	61
<b>4.13</b> High temperatures performance grad vs. limiting temperature at phase angle $30^\circ$ for C and A+ RAP. a) Unaged samples, b) PAV-20 hours aged samples.....	62
<b>4.14</b> High temperatures performance grad vs. limiting temperature at phase angle $45^\circ$ for C and A+ RAP. a) Unaged samples, b) PAV-20 hours aged samples.....	62
<b>4.15</b> Black space diagrams for C and A+ RAP. a) Unaged samples, b) PAV-20 hours aged samples.....	63
<b>4.16</b> Force-Displacement curves at room temperature .....	66
<b>4.17</b> Normalized fracture energies at room temperature and $-10^\circ\text{C}$ . a) C and modified C specimens, b) A and modified A specimens .....	68
<b>4.18</b> Normalized fracture energies at room temperature and $-10^\circ\text{C}$ . a) P and modified P specimens, b) B and modified B specimens.....	68
<b>4.19</b> FI of HMA at room temperature. a) C and modified C mixtures, b) A and modified A mixtures .....	69
<b>4.20</b> FI of HMA at room temperature. a) P and modified P mixtures, b) B and modified B mixtures .....	70

## ***List of Tables***

<b>3.1</b> Prepared asphalts binder blends.....	42
<b>3.2</b> Wavenumber ranges of functional groups.....	44
<b>3.3</b> Components of HMA.....	45
<b>4.1</b> HTPGs of two base asphalt samples .....	49
<b>4.2</b> Carbonyl Indexes for asphalt blends .....	64
<b>4.3</b> Sulfoxide Indexes for asphalt blends .....	64

## *List of Abbreviations*

AASHTO	American Association of State and Highway Transportation Officials
ASTM	American Society for Testing and Materials
BBR	Bending Beam Rheometer
CTOD	Critical crack Tip Opening Displacement
DENT	Double Edge Notched Tension
DSR	Dynamic Shear Rheometer
EBBR	Extended Bending Beam Rheometer
FHWA	Federal Highway Administration
FI	Flexibility index
FTIR	Fourier Transform Infrared
GHG	Green House Gas
HMA	Hot Mixed Asphalt
HTPG	High Temperature Performance Grade
HWY	Highway
I-FIT	Illinois Flexibility Index Test
LVE	Linear Viscoelastic
MTO	Ministry of Transportation of Ontario
MTS	Material Test System
PAV	Pressure Aging Vessel
PEN	Penetration
PET	Polyethylene terephthalate
PG	Performance Grade
PI	Penetration Index
RAP	Reclaimed Asphalt Pavement
RAS	Reclaimed Asphalt Shingles
REOB	Recycled Engine Oil Bottoms
RTFO	Rolling Thin Film Oven
SGC	Superpave gyratory compactor

SHRP	Strategic Highway Research Program
UNCED	United Nations Conference on Environment and Development
UV	ultra-violet

# *Chapter 1*

## *Introduction*

### *1.1 Overview*

Hot Mix Asphalt (HMA) has been a major road construction material for decades, and more than 95 % of worldwide roads are built using asphalt. This is due to the significance of enhancing road in-service performance with its greater economic, structural, and functional benefits. Besides, easy and fast construction, maintenance, and repair activities cause asphalt to lead the pavement construction industry. The most important things to note about HMA are that: 1) it is used in the surface layer of pavement, which receives all traffic and environmental stresses, 2) it is the part of road construction requiring the largest investment of economic resources and 3) the condition of the asphalt mixture on the pavement has a direct influence on the safety of users and most of the indirect costs associated with the use of road infrastructure [1].

Asphalt pavement is subjected to frequent repairs due to the changes in its rheological properties with aging. Hence, existing asphalt pavement materials are commonly removed during resurfacing, rehabilitation, or reconstruction operations [2]. The replacement cost for all municipal roads in Canada is estimated at \$330 billion, of which \$48 billion-worth (15 %) is considered to be in poor or very poor condition, and an additional \$73 billion-worth (22 %) in fair condition [3]. Once removed during rehabilitation or reconstruction of the pavement, the waste produced is called Reclaimed Asphalt Pavement (RAP). Similarly, material removed from aged roofing systems is called Reclaimed Asphalt Shingles (RAS). In this thesis the RAP and RAS acronyms are used to represent the asphalt binders recovered from the actual waste streams that would have contained aggregate, sand and dust.

Significant increases in the cost of asphalt paving and increased awareness of the need for sustainable infrastructure in recent years have in turn increased the use of recycled asphalt

materials (RAP and RAS) in the manufacture of hot-mix asphalt (HMA) [4]. The two primary factors of using RAP and RAS in asphalt pavement are economic savings and environmental benefits. Using RAP and RAS reduces the production cost of new asphalt mixtures by minimizing the virgin material requirements. The use of RAP at rates between 10 % and 40 % makes it possible to achieve savings in manufacturing costs between 9 % and 36 %, respectively [5]. Reclaimed asphalt materials are useful alternatives for virgin asphalt binder. RAP and RAS are most frequently used in Hot Mixed Asphalts production. RAP has become a major recycled material in the United States of America as recycling of asphalt pavement material is an economically and feasible process to rehabilitate old pavements. In the early 1990s, Federal Highway Administration (FHWA) and the U.S. Environmental Protection Agency estimated that more than 90 million tons of asphalt pavement were reclaimed every year, and over 80 percent of RAP was recycled, making asphalt the most frequently recycled material [2]. The economic benefits from the use of RAP materials can provide a great boost to the highway industry by freeing funds for additional highway construction, rehabilitation, preservation, and maintenance [4].

In addition to the economic benefits of using reclaimed asphalt materials, a reduction in the environmental footprint is obtained for the entire road building industry. It is observed that reductions in energy and Green House Gas emission (GHGs) up to 12.2 % with mixtures prepared with 50 % RAP material [6]. Also, the agenda set out in the United Nations Conference on Environment and Development (UNCED) held in Rio de Janeiro (Brazil), 3-14 June 1992, states that increasing energy efficiency, the use of finite resources and minimize waste. This agenda put pressure on production companies including road construction companies. Using of RAP and RAS reduces disposal problems, transportation issues, fuel consumption, and GHG emissions.

However, it is difficult to monitor and regulate the use of RAP and RAS as there is not enough information on how it affects to the performance of neat asphalt and there is lack of protocols to guide constructors on amount of RAP and RAS that should be added to maintain the desirable performance of the road. The belief that pavements constructed with RAP and RAS materials are more prone to cracking than virgin mixtures is generally attributed to stiffening and embrittlement effects induced by attempting to combine weathered, age-hardened materials with virgin materials [4]. Hence, it is critical to consider the properties of the virgin asphalt binder and reclaimed asphalts materials before mixing them.

### ***1.2 Asphalt Cement and Applications***

Asphalt is defined as “dark brown or black cementitious material occurring in nature or obtained by crude oil refining where the predominant material is mainly bitumen” by the American Society for Testing and Materials (ASTM) [7]. The material is commonly called “asphalt” in North America and is referred to as “bitumen” in Europe and Asia. Asphalt is a viscous liquid or a semi-solid adhesive material mainly composed of carbon, hydrogen, sulfur, and oxygen. In addition to the major components, the material contains trace amounts of nickel, vanadium, iron, calcium, and magnesium. Asphalt exhibit relatively complex rheological properties in intermediate temperatures, which acts as a visco-elastic material. At high-temperatures (120 °C – 165 °C), the material act as a Newtonian fluid. Carbon disulfide and many aromatic solvents can be used to dissolve asphalt.

Asphalt cement is the major component in the mixture which determines the quality and longevity of a pavement structure [8]. Over 85 % of the total world asphalt production is used as a binder material in pavement designs for highways, airport runways, car parks, and pedestrian ways. Asphalt pavements are flexible due to the visco-elastic nature of the asphalt material. Around 10 % of asphalt production is used for roofing as the waterproofing quality

of the material. The rest of the production is used in a wide range of industries and sealing purposes in building constructions. For instance, asphalt is used as a water and moisture barrier, erosion controller in the field of agriculture, pipe coating, cable coating, damp proofing, and soundproofing in building constructions. Besides, asphalt is used to construct tennis courts and various types of sport areas.

### ***1.3 Chemical Composition of Asphalt***

Crude petroleum is produced from organic matter which has been subjected to various temperature and pressure changes over millions of years. Asphalt is made from crude petroleum where asphalt contains petroleum derivatives such as carbon and hydrogen. About 90 to 95 percent by weight of asphalt is composed of carbon and hydrogen (80-88 % of carbon and 8-12 % of hydrogen), therefore it is called a hydrocarbon. The hydrogen-to-carbon molar ratio (H/C) is around 1.5. The remaining portion consists of two types of atoms: heteroatoms and metals [9]. Heteroatoms such as sulphur (0-9 %), nitrogen (0-2 %) and oxygen (0-2 %) are generally present. Replacing carbon atoms by the heteroatoms in the molecular structure results in the unique chemical and physical properties of asphalt. Traces of metals are also found, the most numerous being typically vanadium, up to 2000 parts per million (ppm), and nickel (up to 200 ppm) [10].

Asphalt contains complex molecular structures with four major fractions: saturates, aromatics, resins and asphaltenes, commonly known as SARA fractions. Saturates, aromatics and resins belong to the maltene part of the asphalt binder, and asphaltenes can be separated from the maltene as they are insoluble in n-heptane. Fractions in the maltene are separated based on their polarity by using chromatography methods (see Figure 1.1).

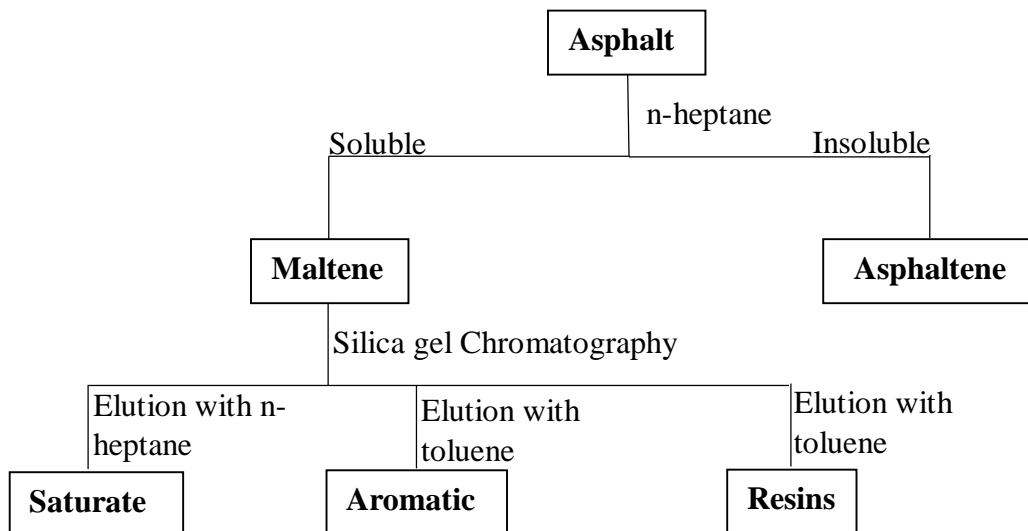


*Figure 1.1: Schematic of (SARA) chromatographic method [11].*

Asphaltene is the highest polar and molecular weight fraction of the asphalt structure and consists of poly-heteroatom aromatic rings. The visco-elastic nature of the asphalt is mainly due to the asphaltene and, typical asphalt binders contain 5–25 % of asphaltene. Asphalt binders with high asphaltene contents are harder at low temperatures and more viscous at high temperatures.

Resins stabilize the asphaltene micelles in the asphalt structure and contain carbon, hydrogen and trace amounts of heteroatoms such as nitrogen, sulfur and oxygen. The fraction is comparatively polar and controls the gel or sol nature of the asphalt binder. Aromatics are non-polar molecules composed of predominantly unsaturated aromatic structures, naphthenic, and paraffinic carbons, and sulfur atoms [12]. About 40 to 65 % of an asphalt binder consists of aromatics and the aromatics fraction functions as the dispersion medium for the resin-peptized asphaltenes. Saturates comprise a 5 to 20 % non-polar fraction in the asphalt binder, including waxy and non-waxy (branched) aliphatic molecules.

### 1.4 Source of Asphalt

World resources of bitumen and heavy oil are estimated to be 5.6 trillion barrels, compared with the remaining conventional crude oil reserves of 1.02 trillion barrels of the heavy oil and bitumen resources and, over 80 % are in Venezuela, Canada, and the U.S.A [13]. The Orinoco Oil Belt of Venezuela is the largest single heavy-oil field comprising 90 % of the World's extra-heavy and heavy oil in place [14]. The largest deposit of natural asphalt is located at Trinidad and Tobago and 'Lake Bermudez' in Venezuela, measuring approximately one hundred acres (41 hectares) and is estimated to be 76 meters deep in the center containing around 10 million tonnes of excess asphalt cement.

The largest oil-sand deposits are in Alberta, Canada, and account for around 70 % of the world's proven bitumen reserves. For North America, the largest heavy oil deposits are in California (77.6 %), Texas (14.6 %) and Alberta (3.3 %), with most of the bitumen resources in Alberta (69.6 %), followed by Utah (12.9 %) and Alaska (7.58 %) [13]. Heavy oil is high density, high viscous crude oil at original reservoir temperature which contains impurities such as waxes and carbon crudes. Oil-sands crudes are a mixture of bitumen, sand and water where bitumen shares the attributes of heavy oil but is even more dense and viscous.



Figure 1.2: Location of the heavy-oil/bitumen deposits in North America [13].

The three major oil sands deposits in Canada are located in the northern half of Alberta, where the largest Athabasca reserve around Fort McMurray is estimated to contain 1,340 billion barrels of crude asphalt of which it is estimated that 10-20 % will ultimately be recoverable [15]. The second-largest deposit is around Cold Lake at the Alberta-Saskatchewan border, which contains 201 billion barrels. The third deposit is near Peace River, located in northwestern Alberta and it is estimated to contain about 157 billion barrels. Out of the total reserve in Alberta, 160 billion barrels are currently recoverable through conventional production (see Figure 1.3) [15].



*Figure 1.3: Locations of the three main oil sands deposits in Northern Alberta [15].*

### ***1.5 Asphalt Specifications***

It is difficult to characterize asphalt performance by using chemical analysis methods as asphalt has a complex chemical structure. Hence, the classification of the asphalt is based on its rheological, physical, and mechanical behavior. Specification of asphalt should provide information on stress handling ability in a traffic condition, the performance of the material under certain geographical conditions and behavior in different climatic conditions, etc. Conventional methods such as penetration grade and viscosity grade tests were used for years, where the penetration test indicates the stiffness of the asphalt, and the grading is based on the

penetrability of the asphalt sample. The viscosity grade is based on the flow behavior of the asphalt sample at 60 °C.

However, conventional testing methods contain limitations. The mentioned methods are empirical, meaning that pavement performance experience is required before the test results yield meaningful information. Any relationship between asphalt penetration and performance has to be gained through experience, whether it is positive or negative [9]. The next limitation is that the relationship between the test and the performance may not be accurate, as most of the time it contains considerable errors. Both penetration and viscosity tests do not provide information on the entire temperature range. Penetration describes only the consistency at a medium temperature (25 °C) while the viscosity test only provides information about higher temperature viscous behavior [9]. There is no way to predict the elastic behavior of asphalt at low temperatures using conventional methods.

Due to the deficiencies of existing conventional methods, the Strategic Highway Research Program (SHRP) began developing new tests for measuring the physical properties of asphalt in 1987 [9], resulting in the new method called Superpave™ Asphalt binder Specifications. The method has a poor correlation with the performance behavior of asphalt in service over the entire temperature range and varying environmental conditions. Besides, the performance of the asphalt binders in various aging conditions has been questioned.

Asphalt binders are more viscous and soft at high temperatures and susceptible to permanent deformation under traffic conditions. Permanent deformation of the pavement structure at high temperatures is called “rutting”. Dynamic Shear Rheometer (DSR) is used to determine the high-temperature grade, which provides the maximum working temperature for asphalt pavement constructions. DSR tests and Double-Edge-Notched Tension (DENT) tests help to obtain the intermediate temperature grade, which provides a better understanding of failures of asphalt pavement at an intermediate temperature range and describes the pavements'

ability to withstand fatigue from road users [8]. Asphalt ability to withstand thermal cracking/low-temperature cracking is given by the low-temperature grade, which can be determined by using a Bending Beam Rheometer (BBR).

Usually, Superpave asphalt binder specifications are expressed using a Performance Grade (PG), designated PG XX-YY, where XX is for the high-temperature limiting temperature and YY is for the low-temperature limiting temperature. For instance, the binder designated as PG 58-28 indicates that the asphalt can resist rutting up to a temperature of 58 °C in summer and limit thermal cracking at low temperatures down to -28 °C in winter [11]. The binder must be used in the environment condition where the maximum average pavement temperature is 58 °C and a minimum average pavement temperature of -28 °C is reached only once every 50 years.

## *Chapter 2*

### *Literature review*

#### *2.1 Aging of Asphalt*

Effects of hardening in asphalt pavements were recognized in the 1900s by pavement engineers and now it has been studied for over 100 years. This hardening process, referred to as asphalt aging, is generally defined as the change in the rheological properties of asphalt binders/mixtures due to changes in chemical composition during construction and in service [15]. Asphalt becomes brittle and stiffer due to aging and this is directly or indirectly connected to asphalt distresses such as thermal and fatigue cracking.

Aging of asphalt binders occurs during the production of asphalt mixtures and while in service when exposed to the surrounding environment [15]. The first stage of aging occurs during the production of HMA, and this aging is rapid and significantly affects the rheological property of asphalt as a thin film of the asphalt layer is exposed to high temperatures. The high temperature during the preparation, hauling and laying of HMA causes a loss of lightweight components that are thermally unstable. The loss of smaller molecules from the asphalt binder increases the viscosity of the sample. The first stage of the aging also referred to as short-term aging is simulated by the RTFO in the laboratory as described in American Association of State and Highway Transportation Officials (AASHTO) standard R 28 [16]. The second stage of the aging occurs during years of service as the pavement is exposed to different climatic events and repeated traffic loading. This aging is referred to as long-term aging, simulated by the PAV in the laboratory and described in AASHTO standard R 28 [16].

Chemical aging due to oxidation is called oxidative hardening. As asphalt composes with organic molecules, asphalt reacts with oxygen in the environment and it changes its structure and the composition. The oxidation reaction occurs at a much faster rate during the

preparation, hauling and laying of HMA while the oxidation rate is relatively slow for in-service pavement, but it happens faster in warmer seasons. Chemical aging causes the brittleness and the stiffness of the asphalt pavement, hence old asphalt pavement are more prone to cracking.

Besides chemical (oxidative) aging there is also a physical phenomenon that occurs in asphalt at cold temperatures. Physical aging of the asphalt is generally thought to be due to wax crystallization, asphalt aggregation, and free volume collapse at low temperatures. Morphology of the asphalt changes with the physical aging and which results in failures of asphalt pavement. Physical hardening is more pronounced at temperatures below 0 °C [9].

## ***2.2 Simulating Asphalt Aging under Laboratory Conditions***

### ***2.2.1 Rolling Thin Film Oven (RTFO)***

The Rolling Thin-Film Oven (RTFO) procedure is used to simulate short term aging of asphalt which occurs during plant mixing, transportation, and placement of HMA. The method can be used to determine the quantity loss of volatile organic materials during the mixing process and RTFO aged samples are used for further testing of physical properties.

In this method, a heated asphalt sample (35 g) is poured into a cylindrical glass jar and the jar is placed horizontally in the circular carriage in a specially designed oven, and the oven temperature must be 163 °C (see Figure 2.1). Then samples are kept under a constant rotation for 85 minutes under hot air injection (4,000 mL/min). The continuous rotation of the bottles keeps the sample homogeneous and dispersed and the method ensures that all the bitumen is exposed to heat and air and the continuous movement ensures that no skin develops to protect the bitumen. In addition, the thin layer that surrounds each bottle makes it possible to simulate the layer of binder that covers the aggregate material [11].

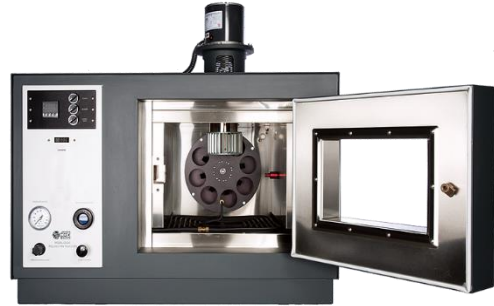
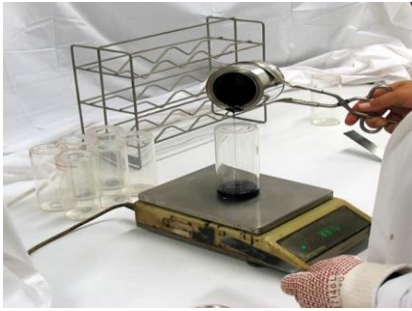


*Figure 2.1: Rolling Thin-Film Oven a) pouring the sample into glass cylinders b) RTFO instrument [17] [18].*

### **2.2.2 Pressure Aging Vessel (PAV)**

The Pressure Aging Vessel (PAV) is used in the laboratory to simulate long-term aging in service (5–10 years) due to different climatic conditions and repeated traffic loading (see Figure 2.2). In the PAV, samples are exposed to a higher temperature and pressure for 20 h, where the standard pressure is 2.08 MPa and the temperature is 100 °C. Air pressure is provided by a cylinder of clean, dry compressed air with a pressure regulator, release valve, and a slow-release bleed valve [9].

Heated RTFO aged samples are poured into PAV pans, and at least 10 pans are placed on a PAV rack. Pan sizes and thickness of asphalt may vary for each test. The rack with the pans is placed in the hot vessel and the lid is quickly closed to avoid the heat loss. After 20 hours of aging, the pressure is released slowly (required 8–10 min) to avoid foaming. Finally, the sample rack is removed from the vessel and pans are stored for further testing.

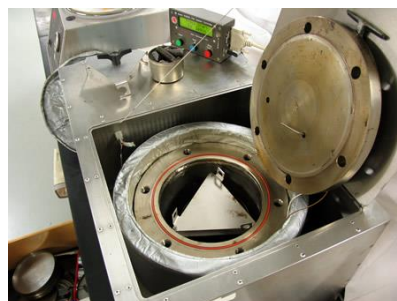


*Figure 2.2: Pressure Aging Vessel [19].*

### ***2.3 Failures of asphalt pavements***

The physical and rheological properties of asphalt mixtures influence pavement performance at high and low ambient temperatures, which in turn can influence the final performance of the mixture [20]. The life time of asphalt pavements is estimated at several decades if properly designed and maintained. However, early failures of asphalt regularly occur due to the thermal stress on the pavement, repeated traffic loadings, heavy loads, chemical contaminations and moisture absorbance. An inappropriate design and poor qualities of mixture material and construction accelerate the aging process of the mixture, leading to early failures that require high maintenance costs, not foreseen in its planning [11].

The two principle structural distress modes (modes of failure) of asphalt pavements are cracking and permanent deformation (rutting). The two types of cracking are fatigue cracking and thermal cracking (low-temperature cracking). Besides, moisture damage is also a major factor to early failures of asphalt pavements.

#### ***2.3.1 Permanent Deformation (Rutting)***

Permanent deformation, also known as rutting, is one of the major distresses in the asphalt pavement. This is non-recoverable and mainly depends on slow traffic at high temperatures, repetitive traffic load, and weather conditions. Quality of the mixture and construction is also crucial for rutting performance. Rutting, usually occurring in both asphalt layers and underlying unbound layers [21], often appears in a form of surface depression in wheel paths (see Figure 2.3) , especially in intersections and bus stops of urban roads, and horizontal loading created by tire friction during frequent vehicle braking and accelerating actions [21]. Many problems are associated with rutting, such as further deterioration of the pavement due to the water intrusion into the pavement structure through the ruts and the hydroplaning safety hazard with accumulating water in the ruts.

Shear flow deformation is the primary cause of rutting in asphalt pavement layer [22]. The Superpave specification defines and places requirements on a rutting factor,  $G^*/\sin \delta$ , which represents a measure of the high temperature stiffness or rutting resistance of the asphalt binder [9]. Both  $G^*$  and  $\sin \delta$  can be measured by the DSR. According to the Superpave specifications, the  $G^*/\sin \delta$  value should be kept at a minimum of 1.00 kPa for unaged binders and the value should be a minimum of 2.20 kPa for RTFO aged binders, in order to have a sufficient rutting resistance in the asphalt pavement. It is shown that higher  $G^*$  values and lower  $\delta$  value are considered desirable attributes from the standpoint of rutting resistance [9]. Hence, stiffer and elastic binders are considered to have higher rutting resistance.



*Figure 2.3: Rutting on asphalt pavement [23].*

### **2.3.2 Fatigue Cracking**

Fatigue has been defined as “the phenomenon of fracture under repeated or fluctuating stress, having a maximum value less than the tensile strength of the material” [24]. This distress is induced over extensive traffic repetitions at moderate temperatures that are typically in the 15 °C to 30 °C range. Catastrophic failure throughout the pavement can be seen after the initiation and propagation of fatigue cracking (see Figure 2.4). Generally, the distress has three stages that are described as crack initiation, crack propagation, and disintegration. Crack

initiation is the stage where new micro-cracks develop, crack propagation is the development of micro-cracks up to giant cracks, and disintegration is the final failure of the material due to the growth of the unstable cracks.

Fatigue cracks are believed to either initiate at the bottom or top of the asphalt layer then propagate upwards or downwards, respectively [25]. Usually, fatigue cracks propagate from base to top in thin pavement layers while the cracks originate from the surface in thick pavement layers and propagate downwards. Factors responsible for fatigue cracking besides repeated traffic are inadequate compaction, heavy loads, poor subgrade drainage, and improper pavement layer design, and are common.

$G^*$  and  $\delta$  from DSR analysis are used to evaluate the fatigue resistance of the asphalt binder. Since fatigue generally occurs at low to moderate pavement temperatures, after the pavement has been in service for a period of time, the specification addresses these properties using binder aging in both the RTFO and PAV [9].  $G^* \cdot \sin\delta$  is the parameter for fatigue resistance and the maximum value should be 5,000 kPa for  $G^* \cdot \sin\delta$  according to the Superpave binder specification. Hence, lower values for  $G^*$  and  $\delta$  desirable for fatigue resistance according to the specification. Thus, the Superpave specification promotes the use of compliant, elastic binders (PAV aged) of low stiffness to address fatigue cracking [9]. However, this has not been proven to work very well as many oil modified binders are seen to fail early and severely.



*Figure 2.4: Fatigue cracking [26].*

### ***2.3.3 Thermal Cracking***

Thermally induced cold temperature cracking of asphalt pavement is a problem in northern climatic regions as well as in areas which experience large extremes in daily temperatures such as mountainous regions [27]. This failure is prominent in the United States, Canada and other areas at extreme northern and southern latitudes. Low temperatures responsible to the thermal cracking due to differential thermal contraction, an instant drop in surface temperature of more than 9.5 °C (15 °F) can result in the development of cracks, due to surface contractions [28]. If the thermal stress is equal to or greater than the tensile strength of the pavement, a micro-crack may develop on the pavement surface, and, after additional low temperature cycles, this crack will propagate downward through the pavement [27]. Low temperature cracking is also associated with the volumetric changes of the asphalt layer. Thermal stress in the surface develops when the pavement tends to contract its volume with the temperature drop while keeping the thermal strains unrealized, which leads to the formation of cracks in order to release these tensions.

It is observed that there are three major stages of low temperature cracking. First, the thermal stress exceed the tensile strength of the pavement. Next, cracks develop due to the temperature fluctuations and shrinking. Eventually, cracks propagates though the pavement due to the freezing and shrinking of the sub base of the asphalt pavement. Usually, the cracking pattern is perpendicular to the direction of the vehicular movement and patterns can be observed in regular intervals (see Figure 2.5)

Several investigations have shown that binder consistency parameters such as stiffness, viscosity, penetration and softening point have a strong influence on low temperature cracking of asphalt mixtures [27]. Besides pavement design, the age of the pavement, the thickness of the layer, less absorptive aggregates, and traffic load etc. are associate with the thermal

cracking. In AASHTO standard M 320, the main way of examining the propensity of an asphalt binder to develop thermal stresses at a specified temperature is to use data generated from the bending beam rheometer (BBR) [9]. Since low temperature cracking usually occurs after the pavement has been in service for some time, this part of the specification addresses these low temperature properties using asphalt binder that has been aged in both the RTFO and PAV [9].

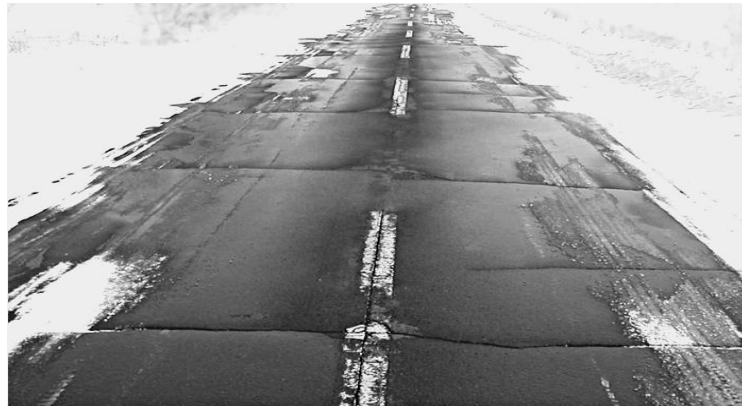


*Figure 2.5: Low temperature cracking [29].*

#### **2.3.4 Moisture damage**

Durability of asphalt pavements highly depends on environmental factors such as temperature and humidity. Moisture damage, commonly referred to as stripping, can be defined as the loss in strength and durability of the asphalt mixture in the presence of water. This failure of the asphalt mixture is a complicated mode of asphalt pavement distress, which is due to the loss of the adhesive bond between the asphalt layer and the aggregates with the intrusion of water. So, it has been suggested that the adhesion between aggregate and bitumen in the dry condition and its degradation with the presence of water are two main attributes that determine the moisture sensitivity of pavements [30].

Moisture sensitivity of the asphalt mixture related to the pavement materials (surface texture of aggregates and chemical composition of asphalt), mixture design (air void level, thickness, and permeability) and environmental factors and pavement age.

Anti-stripping additives such as Portland cement and hydrated lime are used to avoid stripping in the asphalt mixture. The additives minimize the stripping by increasing the physico-chemical bond between the bitumen and aggregate and improving the wetting by lowering the surface tension of the bitumen. For the well-coated aggregate, it is hard for water to penetrate the aggregate–bitumen interface to break the aggregate–bitumen bond [30].



*Figure 2.6: Moisture damage [31].*

#### ***2.4 Conventional Testing Methods for Asphalt Binder***

Penetration, softening point, and viscosity test methods are the most common conventional test methods that have been used from the 1900s. Tests are empirical and used to evaluate the stiffness and the viscosity of asphalt binders. Above conventional tests are important to specify penetration grade, oxidized grade, cutback, and the hard grade where penetration grade is the most important in road constructions. Softening point tests and penetration tests are used to determine the penetration grade and, viscosity tests and softening point tests are used to predict oxidize and hard grades. Cutback grade can be determined by the viscosity test. However, these test methods cannot be used to evaluate some engineering properties of asphalt (e.g., strain and stress), and there are no relations of the test results with the service performance.

##### ***2.4.1 Penetration Test***

The original penetration test was introduced by H.C. Bowen of the Barber Asphalt Paving Company in 1888 and the test is the oldest and widely used method. The purpose of the

test is to measure the consistency/hardness of the asphalt binders in specific testing conditions. Stiffness of the asphalt binder at low temperatures and viscosity at the high temperature of the binder can be approximately predicted by using the penetration grade.

Temperature, time, and the load on the needle are the basic considerations where 25 °C temperature, 5 s time, and 100 g of load are commonly used as standard conditions. The unit of the penetration measurement is decimillimeters, which is denoted as dmm where 1 dmm is equal to 0.1 mm (millimeter). For instance, the meaning of 50 PEN (penetration) is, the needle penetrates 50 dmm under a 100g load at 25 °C. Harder asphalt at 25 °C has lower penetration while soft asphalt at 25 °C has comparatively high penetration.

Penetration related to the temperature and the relationship is given by the following equation.

$$\log P = AT + K \quad (1)$$

Where, P = penetration of the needle, A= temperature susceptibility, which is defined as the Penetration Index (PI), T is the testing temperature and K is a constant.

To have the Penetration Index (PI), the following equation is used,

$$PI = \log \frac{(Pen@T1 - Pen@T2)}{T1 - T2} \quad (2)$$

Here, the denominator is the difference of two different temperatures (T1 and T2) and the numerator is the difference of two penetrations values at T1 and T2. PI values can be used to evaluate the stiffness of the binder at any temperature [32].

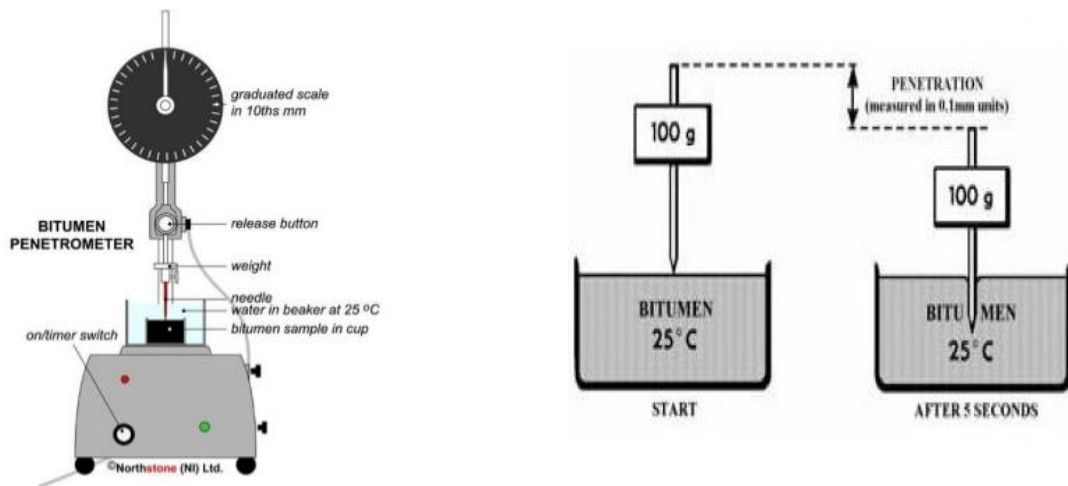


Figure 2.7: Penetration test [33].

#### 2.4.2 Ring and Ball Softening Point Test

The softening point test has existed since the early 1900s, and can be used to determine the consistency/hardness of the penetration and oxidized grade asphalt binders. As asphalt is a viscoelastic solid, asphalt converts to a viscous liquid from an elastic solid when increasing the temperature of the asphalt binder sample. Asphalt does not have a clearly defined melting point, and is gradually softening with the increasing temperature. The softening point test indicates the asphalt's tendency to flow at elevated service temperatures [8].

The apparatus called “ring and ball” is used to conduct a softening point test and the commonly used temperature range is 30 °C to 157 °C as the asphalt softening point often appears within the particular temperature range (see Figure 2.8). The liquid medium for the test depends on the estimated softening point of the testing asphalt binder sample. If the estimated softening point is lower than the 80 °C, water is used as the liquid medium while if the softening point is higher than 80 °C glycerin is used as the liquid medium.

The softening point test according to the ASTM D 36-95 involves placing a steel ball of weight 3.5 g in a solidified asphalt sample contained in a brass ring [34]. The system is

immersed in the liquid medium and gradually increase the temperature of the medium at a constant rate (5 °C per minute). The binder becomes soft with the increasing temperature and the weight cannot withstand further by the asphalt sample. As a result of that, asphalt falls onto the base place which is 25 mm below to the ring position. Temperature is recorded once asphalt touches the base plate, and this temperature is called softening point temperature.

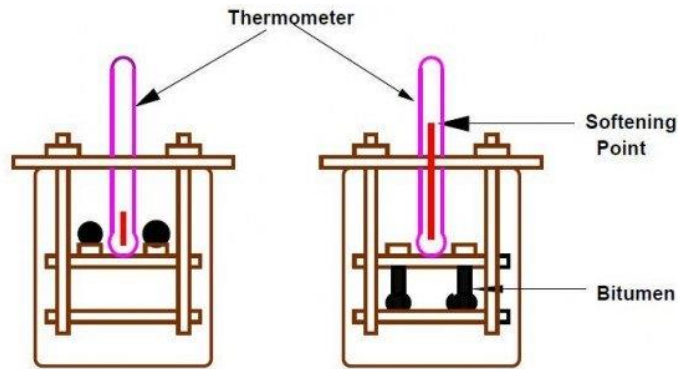


Figure 2.8: Ring and Ball Apparatus [35].

### 2.4.3 Viscosity Test

Viscosity is a basic property of asphalt and the viscosity measurement test provides the resistance to flow of asphalt binder in a temperature or a range of temperature. It is a measure of the resistance to flow. The higher the viscosity of liquid bitumen, the more nearly it approaches a semi-solid state in consistency [36].

There are two types of viscosities are often measured, the dynamic viscosity and the kinematic viscosity. Dynamic viscosity is defined as the ratio between the applied shear stress and induced shear rate of a fluid [32] and the kinematic viscosity is the ratio between dynamic viscosity and the density of the fluid (Equation 3 and 4).

$$\text{Dynamic viscosity} = \frac{\text{Applied shear stress (Pa)}}{\text{Induced shear rate (Per S)}} \quad (3)$$

According to the equation, the SI unit for dynamic viscosity is Pascals multiplied by seconds (Pa.s). The relationship between the applied shear stress and the induced shear rate is not linear for non-Newtonian fluids like asphalt.

$$\text{Kinematic viscosity} = \frac{\text{Dynamic viscosity}}{\text{Fluid density}} \quad (4)$$

Kinematic viscosity is measured in  $\text{m}^2 \cdot \text{s}^{-1}$ . The 135 °C measurement temperature was chosen to simulate the mixing and laydown temperatures typically encountered in HMA pavement construction [37]. The vacuum capillary or Brookfield viscometers are used for asphalt viscosity measurement depending on the specification required (see Figure 2.9) [8].

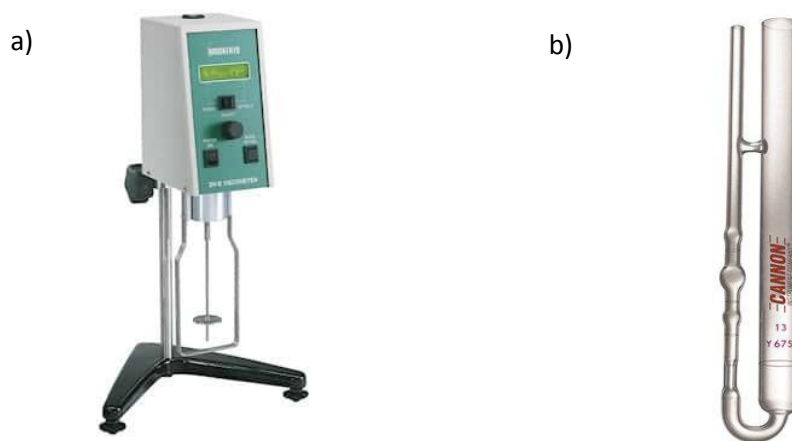


Figure 2.9: a) Brookfield viscometer and b) Vacuum capillary viscometer [25] [26].

## 2.5 Superpave Testing Methods

In 1987, the U.S. Congress established a 5-year, \$150 million applied research program aimed at improving the performance, durability, safety, and efficiency of the nation's highway system, called the Strategic Highway Research Program (SHRP) [40]. This program was officially authorized by the Surface Transportation and Uniform Relocation Act of 1987 and consisted of research concentrated in four key areas: asphalts, concrete and structure, highway

operations and pavement performance. More than hundred devices has been introduced by the SHRP when it was closed at 1993.

The area of asphalt considered the research and development of new approaches to HMA designs. Assessing, protecting and rehabilitating concrete pavements and structures were observed and investigated by the concrete and structures area. The area of highway operations was used to investigate on pavement preservation, work zone safety and snow and ice control while a long term pavement performance program was conducted under the area of pavement performance (A 20-year study of over 2,000 test sections of in-service U.S. and Canadian pavements to improve guidelines for building and maintaining pavements [40]).

### ***2.5.1 Fourier-Transform Infrared (FTIR) Spectroscopy***

Functional groups available in a material affect the physical and chemical behavior of that material. Hence, identifying the changes of functional groups and changes in the proportion of functional groups of asphalts by adding reclaimed asphalts and the aging process of asphalt, which is helpful to predict and explain the changes of the physical and chemical behavior of asphalt binders. As asphalt binders contain complex chemical structures, it is difficult to study the entire chemical composition of the asphalt binders. However, the availability of C, H, O, N, S, and some trace amounts of metals are already identified.

Asphalt failures are mainly due to oxidative aging. Oxidative aging can happen when the asphalt is exposed to air and ultra-violet (UV) radiations during mixing, compaction, transportation, and in-service period. Air and UV radiation exposure of asphalt results in the increment of the proportion of carbonyl and sulfoxide in the asphalt structure. A high amount of carbonyl and sulfoxide cause the stiffness and the brittleness of the asphalt binder. Hence, the determination of carbonyl and sulfoxide content of the structure explains the oxidation level of the asphalt.

Transmission and reflection FTIR modes are commonly used for asphalt characterization. In transmission mode, the IR beam passes through the sample. It requires a time-consuming preparation of very low thickness bitumen films or may need the use of a solvent [41]. In reflection mode, the beam enters a crystal with high refractive index held in contact with the sample [41].

The carbonyl (C=O) area is commonly defined as the band around the 1680 cm<sup>-1</sup> peak, whereas the sulfoxide (S=O) area is the band around 1030 cm<sup>-1</sup>. The aliphatic group (symmetric and asymmetric bending vibrations around 1460 and 1376 cm<sup>-1</sup>, respectively) is commonly used as a reference group, since it is anticipated that these structures are stable and not affected by applied ageing procedures [42]. In order to minimise the influence of sample thickness and IR radiation path length, the general principle is to normalize the absorption values  $V(1030)$  and  $V(1700)$  obtained for these specific wave numbers by calculating a ratio of a value obtained at a reference wavenumber  $V(v_{ref})$  which is supposed not to be significantly affected by oxidation [41]. Usually, the ethylene group wavenumber is considered as the reference wave number. The following equations are used to obtain carbonyl ( $I_{co}$ ) and sulfoxide ( $I_{so}$ ) indexes.

$$I_{so} = \frac{V(1030)}{V(ref)}$$

$$I_{co} = \frac{V(1700)}{V(ref)}$$

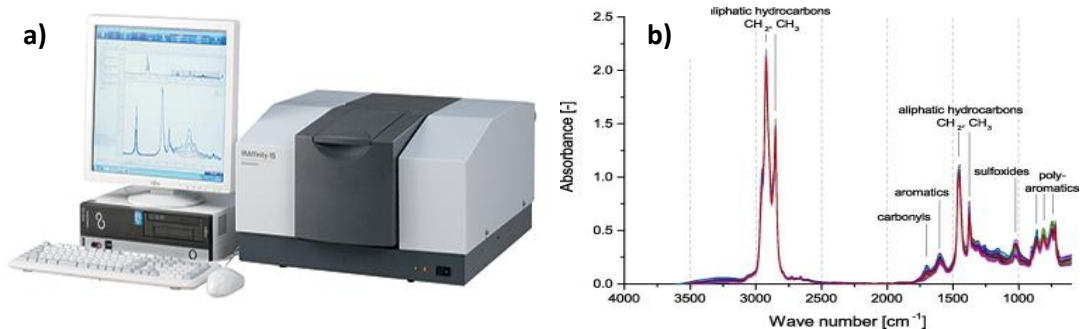


Figure 2.10: a) FTIR spectrometer b) Sample FTIR spectrum for asphalt [43] [44].

### 2.5.2 Dynamic Shear Rheometer (DSR)

The Dynamic Shear Rheometer is used to evaluate the asphalt behavior on both temperature and loading time, two factors which are related to the asphalt behavior and should be included in asphalt tests. As DSR is able to predict both factors simultaneously, the testing equipment was described as the ideal to address both loading time and temperature dependency of asphalt behavior. DSR tests determine the flow behavior / rheology of asphalt at intermediate temperatures to high temperatures by quantifies rheological properties such as complex modulus ( $G^*$ ) and phase angle ( $\delta$ ) of the material. The complex modulus magnitude and phase angle are often the two parameters that represent the Linear Viscoelastic (LVE) rheological properties of bitumen [45].

$G^*$  represents the stiffness of the material, where  $G^*$  is the measure of the total resistance of a material to deformation when exposed to repeated pulses of shear stress [9].  $G^*$  is given by the equation 5, and  $G^*$  has two components: elastic (recoverable) and viscous (non-recoverable) where the elastic component is represented by the storage modulus ( $G'$ ) and the viscous component is represented by the loss modulus ( $G''$ ). The phase angle ( $\delta$ ) is an indicator of the relative amounts of recoverable and non-recoverable deformation and  $\delta$  is also defined as the phase difference between stress and strain in harmonic oscillation (see Figure 2.12) [9, 45].  $\delta$  is equal to  $90^\circ$  when the material is purely viscous and the  $\delta$  is  $0^\circ$  when the material is purely elastic.  $\delta$  is in between  $0^\circ$  and  $90^\circ$  in the viscoelastic range of the material.

$$\text{Complex modulus} = \frac{\text{Peak shear stress}}{\text{Peak shear strain}} \quad (5)$$

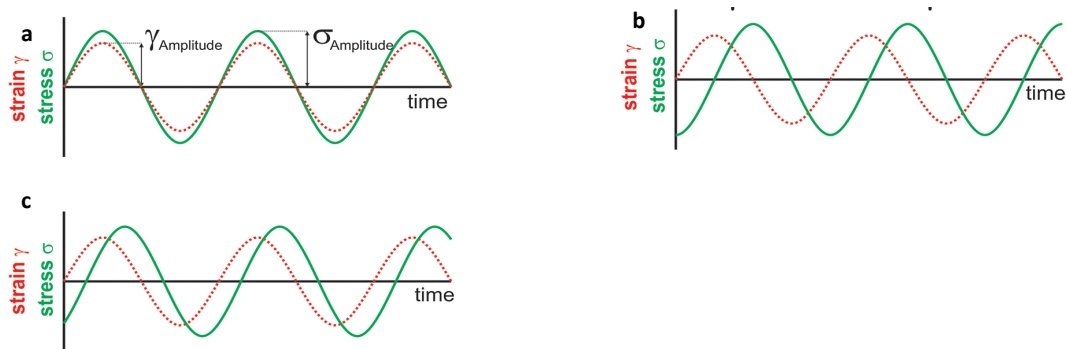


Figure 2.11: Stress-strain response during oscillatory testing. a) Purely elastic response, b) purely viscous response and c) viscoelastic response [46].

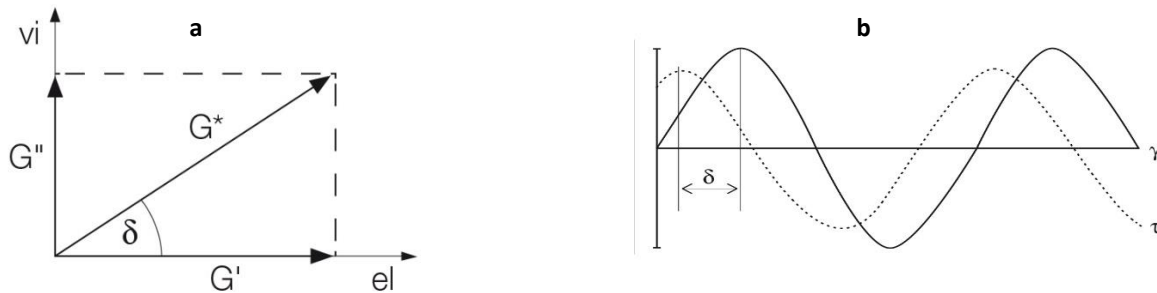


Figure 2.12: Representation of phase angle ( $\delta$ ). a)  $\delta$  as an indicator of the relative amounts of recoverable ( $G'$ ) and non-recoverable ( $G''$ ) deformation and b)  $\delta$  as the phase difference between stress and strain in harmonic oscillation [47][48].

In a DSR test, the temperature chamber and connected nitrogen vessel regulate the temperature of the sample, and the motor and the bearing system are controlled by the compressor. Output of the DSR test is displayed by the computer with the DSR software.

The basic DSR operation consists of placing bitumen between two parallel plates, one that is fixed (stator) and the other that oscillates (rotor) (see Figure 2.13) [46]. Plates with 8 mm diameter and 25 mm diameter are commonly used where the 8 mm parallel plate configuration is used to conduct intermediate temperature range DSR tests and the 25 mm parallel plates configuration is used to conduct high temperature range DSR tests. The

thickness of the sample is 2.0 mm and 1.0 mm for 8 mm parallel plate configuration and 25 mm parallel plate configuration respectively.

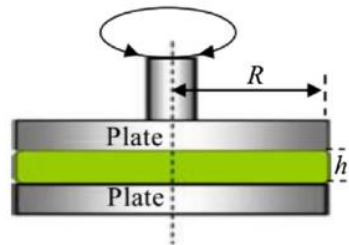


Figure 2.13: Representation of parallel plate configuration of DSR plates.

Testing is performed by oscillating the spindle around its own axis point “O” such that a radial line through point “A” moves to point “B”, then reverses direction and moves through point “A” to point “C”, followed by moving back from point “C” to point “A” [46].

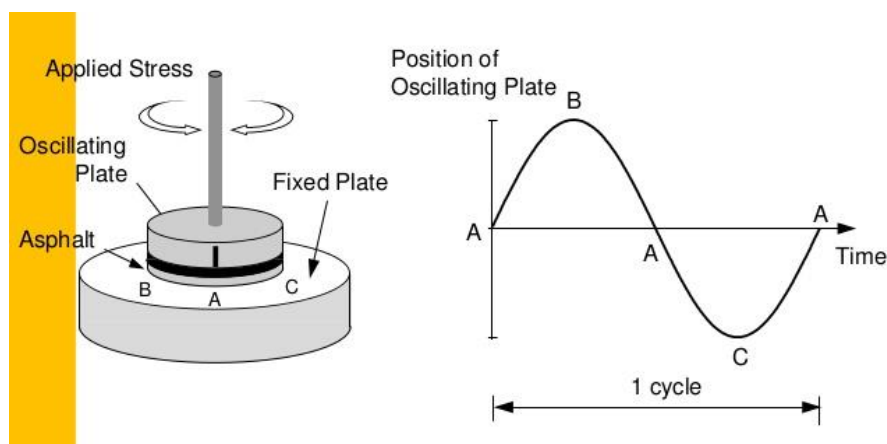


Figure 2.14: Schematic representation of DSR operation [49].

Two forms of  $G^*$  and  $\delta$  are used in the Superpave binder specification [9]. Asphalt susceptibility of permanent deformation/rutting and fatigue cracking can be evaluated by parameters  $G^*/\sin \delta$  and  $G^* \sin \delta$ , respectively. The minimum value  $G^*/\sin \delta$  must be 1.00 kPa for unaged asphalt binder and 2.20 kPa for RTFO aged asphalt binders. The maximum of  $G^* \sin \delta$  parameter should be 5,000 kPa for PAV aged asphalt samples.



*Figure 2.15: DSR Instrument [50].*

### **2.5.3 Bending Beam Rheometer**

The philosophy behind the BBR and AASHTO M 320 (2002) specification dates back to work from the 1950s and 1960s, when researchers at Shell Laboratories in Amsterdam found a reasonable correlation between the binder stiffness at a fixed loading time and various failure properties in the binder and mixture [51]. The BBR test method was introduced to the engineering field during the Strategic Highway Research Program (SHRP) in order to address low temperature performance of asphalt binders. The instrument measures the amount of deflection that can be imposed on a beam of asphalt under a constant load at temperatures that corresponds to its minimum pavement service temperature when asphalt behaves as an elastic solid [34]. BBR is an ideal candidate for the purpose as it contains desirable features such as low conditioning time, limited use of the material, availability, rugged-testing and the instrument has a user friendly calibration verifications.

The BBR test method measures two parameters: flexural creep stiffness  $S(t)$  and stress relaxation capacity ( $m(t)$ ) of asphalt. Creep stiffness is the measure of the resistant of an asphalt binder under a constant load and stress relaxation capacity, and is given by the slope of the creep stiffness master curve at 60 seconds, where  $m$  is also known as the creep rate. The tests

are commonly conducted with PAV aged asphalts under laboratory conditions as thermal cracking/low temperature cracking often occurs with old asphalt pavements. The AASHTO M 320 standard protocol (2002) provides the specification criteria, to pass or fail the BBR test. The asphalt sample is acceptable when the  $S(t)$  is equal or lower than 300 MPa and m-value is equal or greater than 0.3. An asphalt sample with a higher  $S(t)$  value and a lower m-value than the standard limits (300 MPa and 0.3, respectively) are more brittle and prone to thermal cracking.

According to standard specifications, a 125 x 12.5 x 6.25 mm asphalt beam is preconditioned at +10 °C and +20 °C above the designated low pavement temperature in an ethanol bath for an hour. The load is then applied at a designated low payment temperature in an ethanol bath, and the defection of the beam is evaluated concerning time.

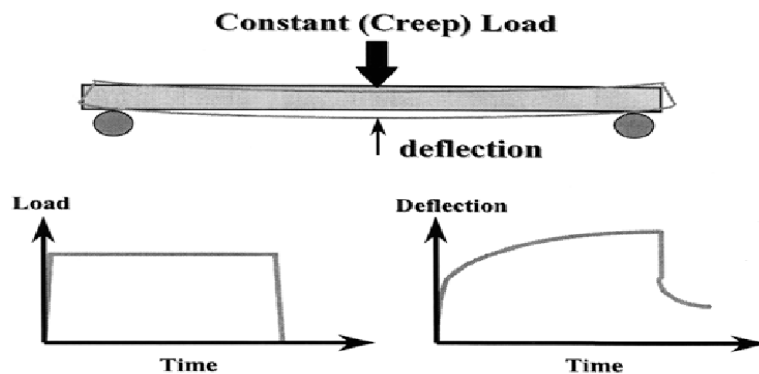


Figure 2.16: Deflection measured against time in the BBR test [52].

Flexural creep stiffness  $S(t)$  is calculated by following equation,

$$S(t) = \frac{PL^3}{4bh^3\delta(t)} \quad (6)$$

Where,

$P$  = applied constant load (100 g)

$L$  = distance between beam supports (102 mm);

$b$  = beam width (12.5 mm);

$h$  = beam thickness (6.25 mm)

$\delta(t)$  = deflection at a specific time (60 s).

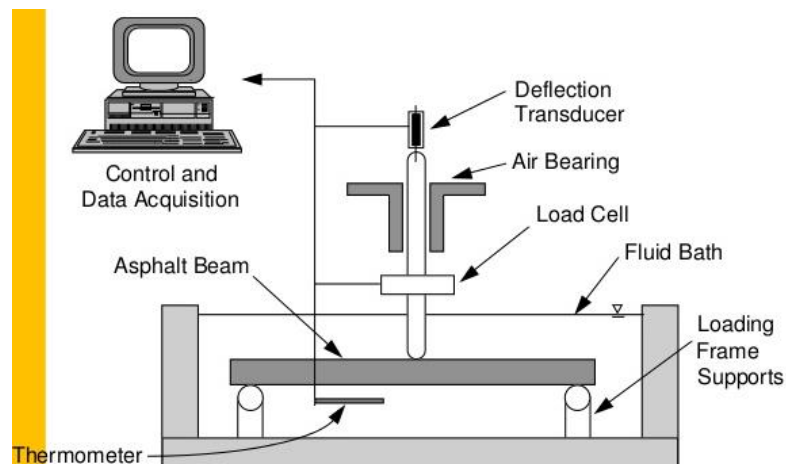


Figure 2.17: Bending Beam Rheometer [53].

## 2.6 Ministry of Transportation of Ontario (MTO) Methods

Enhanced binder grading methods were introduced by the Ministry of Transportation of Ontario (MTO), in collaboration with Queen's University. MTO has found that some problems with the Superpave specification system relate to the practical implementation. Evidence from pavement trials in Ontario and elsewhere and from incidents of premature cracking in major MTO contracts has shown that there is room for improvement [54]. The major shortcomings of the Superpave specification system are identified as follows:

- (1) Insufficient ageing in the RTFO and PAV,
- (2) Insufficient conditioning in the BBR and,
- (3) Absence of fracture/failure tests for the brittle and ductile states.

Extended BBR LS-308 and the Double Edge-Notched Tension (DENT LS-299) have been developed to address deficiencies and it is proven that these new methods are more

successful at predicting the true low temperature performance of asphalt, and the tests show good reproducibility in the laboratory conditions.

### ***2.6.1 Extended Bending Beam Rheometer (EBBR)***

The objective of using EBBR protocols is to evaluate the susceptibility of asphalt binder to thermo-reversible aging. The sample is exposed to cold temperatures for a more extended period in the EBBR test method than in the regular BBR test method. This is meant to induce long-term physical hardening conditions which are similar to the long-term exposure of the asphalt pavement to the harsh low-temperature conditions, especially during winter [34]. One hour conditioning period in regular BBR test is believed to be insufficient to simulate in service pavement conditions. Hence, 1, 24 and 72 h of conditioning are used in the EBBR test. Besides, instead of a single conditioning temperature for the regular BBR test, two conditioning temperatures are used in the EBBR method. Conditioning temperatures are selected depending on the lowest designated temperature for the pavement ( $T_{\text{design}}$ ): 10 °C and 20 °C above  $T_{\text{design}}$ .

The lowest limiting temperature and the worst grade loss are determined after the EBBR test. According to LS-308, the worst grade loss should be under 6 °C compared to the regular BBR test after the EBBR test with 72 h of conditioning time. The EBBR is reliable test as the accuracy is around 95 % in terms of predicting the low-temperature behavior of asphalt binders.

### ***2.6.2 Double-Edge-Notched Tension (DENT) Test***

The LS-299 DENT protocol determines the essential and plastic works of failure ( $w_e$  and  $\beta w_p$ , measures of strength and toughness, and an approximate Critical Crack Tip Opening Displacement (CTOD), a measure of strain tolerance) [55]. The essential work of failure,  $W_{\text{essential}}$ , represents the total work necessary to separate two failure surfaces in a localized area of a specimen under high constraint. The plastic work,  $W_{\text{plastic}}$ , is the work dissipated away from the failure zone, and as such is less important in the failure of an asphalt mixture where cracks are typically highly localized in between large aggregate particles [55].

$$W_{total} = W_{essential} + W_{plastic} \quad (7)$$

Where  $W_t$  is the total work, the unit is performed in J for  $W_{total}$ ,  $W_{essential}$  and  $W_{plastic}$ .

$W_{essential}$  and  $W_{plastic}$  is determined by following equations 8 and 9 respectively,

$$W_{essential} = w_e \cdot LB \quad (8)$$

$$W_{plastic} = w_p \cdot \beta L^2 B \quad (9)$$

Unit is performed in  $J/m^2$  for both  $w_e$  and  $w_p$ .

$w_e$  is specific essential work of failure and  $w_p$  is specific plastic work of failure.

$L$  is the ligament length in the DENT specimen (m),  $B$  for the thickness of the sample (m) and

$\beta$  is the shape factor of the plastic zone, which is geometry dependent.

Total work can be also performed in equation (10)

$$W_t = (w_e \cdot LB) + (w_p \cdot \beta L^2 B) \quad (10)$$

Cross section area of the plastic zone =  $LB$ , equation (10) can be obtained by dividing equation

(11) by  $LB$  ( $W_t/LB = w_t$ )

$$w_t = w_e + w_p \cdot \beta L \quad (11)$$

Here  $w_t$  is specific total work of failure ( $J/m^2$ ).

The above relationship allows for the determination of the specific essential work of failure,  $w_e$  by plotting the total specific work of failure,  $w_t$ , versus the ligament length,  $L$ . The intercept provides  $w_e$  and the slope provides a measure of the specific plastic work of failure,  $w_p$ , times the  $\beta$  constant [34, 55].

CTOD is obtained by dividing  $w_e$  by the net section stress in the specimen with the smallest ligament length ( $\delta_{nt, 5mm}$ )

$$CTOD = w_e / \delta_{nt, 5mm} \quad (12)$$

To conduct the DENT test, a hot asphalt sample is poured into a silicon mold between aluminum inserts with ligaments lengths of 5 mm, 10 mm, and 15 mm, and is kept in a water

bath for 3 hours which has a constant temperature (15 °C). The conditioned samples are then stretched at a loading rate of 50 mm/min until a fracture occurs (see Figure 2.18) [56].

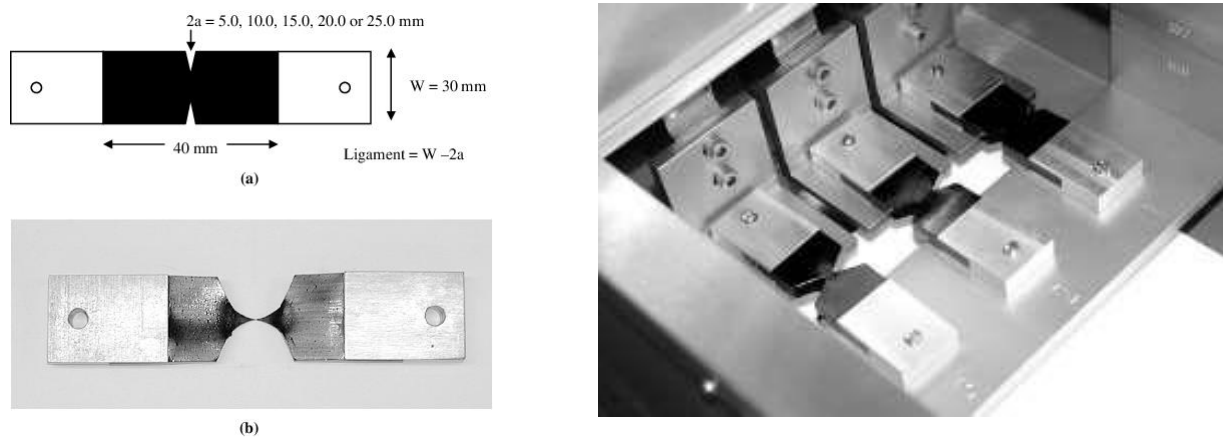


Figure 2.18: Double-Edge-Notched Tension (DENT) design [57] [58].

## 2.7 Hot Mix Asphalt (HMA) Testing

### 2.7.1 Superpave Gyrotory Compactor (SGC)

The SGC is used to simulate the field HMA asphalt compaction process in the laboratory. The instrument was developed under the SHRP program in the late 1980s and early 1990s as part of the Superpave mix design system. At present, the SGC is used in many countries including Canada and the USA. Four important factors are considered when using the SGC to prepare HMA specimens: the pressure applied to the specimen during compaction; the speed of gyration/rotation; the number of gyrations applied to the specimen; and the angle of gyration. Experience has shown that pavements that maintain an air void level of around 4 percent provide the best long-term performance in the field. As a result, choosing the appropriate level of compaction in the laboratory is crucial in designing a well-performing mixture [59]. The SGC was designed with 150 mm (6 inch) molds to be capable of accommodating large aggregates [59].

The mold and the top plate are placed in an oven set at the compaction temperature approximately for 45 to 60 min before compaction. Depending on the SGC make and model, the following steps will either be performed automatically after pressing a “start” button or be initiated by the user [59]; lower the loading ram until it reaches the pressure of 600 kPa, apply the 1.16° angle and proceed with gyrations to the preset number. The height of the specimen is regularly monitored throughout the compaction process and the ram loading system maintains the pressure of 600 kPa.



*Figure 2.19: Pine Instruments Superpave Gyrotory compactor (SGC) [60].*

### **2.7.2 Illinois Flexibility Index Test (I-FIT)**

The I-FIT is a simple and cost effective test method which was developed using the work to fracture principle. A semi-circular bending (SCB) specimen with a vertical notch along the symmetric axis is used to determine the fracture resistance of an asphalt mixture. The provisional standard test method, AASHTO TP-124, “Determining the Fracture Potential of Asphalt Mixtures Using the Semi-Circular Geometry at Intermediate Temperature,” calls for 50-mm thick, 150-mm diameter semi-circular specimens to be tested using a three-point bending principle, at the constant displacement rate of 50 mm/min [61]. The specimen is conditioned at the test temperature for 2 h before the test. A force-displacement curve is obtained from the I-FIT and one of the primary outputs of the test is the fracture energy ( $G_f$ ),

which represents the energy dissipated by the crack propagation (see Figure 2.20). This parameter is calculated as the area under the load-displacement curve divided by the area of the crack that propagates during testing [61].

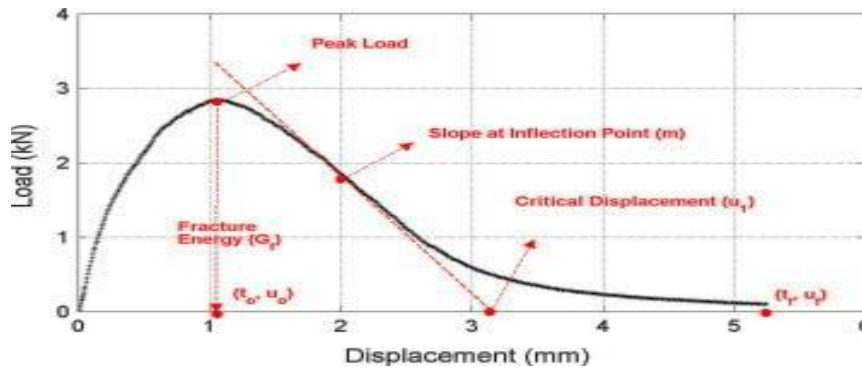


Figure 2.20: Force-displacement curve in I-FIT [62].

The Flexibility Index (FI) is calculated by using fracture energy ( $G_f$ ) and slope at inflection point ( $m$ ). The FI is thought to be a good indicator to asphalt pavement cracking performance, which is used for determine overall resistance of asphalt pavement to crack propagation. Further, the FI value is used to distinguish differences in asphalt mixture properties, and it has been reported that the FI has an excellent discrimination potential when analyzing laboratory-produced asphalt mixtures that contain high levels of recycled materials and long aging times [61]. According to Ozer et al., asphalt mixtures show excellent cracking resistance if they have a FI value above 10, and show a comparatively poor cracking resistance if they have an FI value below 6.

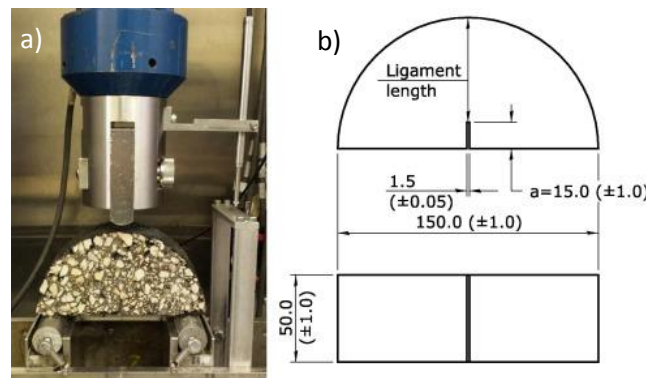


Figure 2.21: a) SCB test specimen and configuration and b) geometry of specimen (dimensions are in millimeters) [62].

$$G_f = \frac{W_f}{A_{lig}} \quad (13)$$

$W_f$  - The work of fracture (Joules), calculated as the area under the load vs. load line displacement curve,  $G_f$ - fracture energy (Joules/m<sup>2</sup>) and  $A_{lig}$  - ligament area.

$$FI = \frac{G_f}{|m|} A \quad (14)$$

FI- Flexibility Index,  $|m|$  - Absolute value of slope at inflection point (m) and A is used for unit conversion and scaling (A= 0.01).

## **2.8 Modification of Asphalt**

Different modifications of asphalt binders have been introduced as the result of the increasing demand for higher performance asphalt. Improved life span and higher resistance for asphalt failures such as rutting, fatigue cracking, and thermal cracking are expected by the modifications. By properly choosing the feedstock and processing conditions, it is possible to produce high-performance bitumen with the correct balance in chemical composition, molecular weight distribution, and physical characteristics [63]. But, controlling the chemical composition while the manufacturing process has become extremely difficult. To address the difficulties, a number of additives are used to modify asphalt binders. Polymers are prominent among those and polymer modification is one of the succeeding methods and widely used. In addition, mineral oils, fibers, sulfur, etc. are employed as additives.

Both synthetic and natural polymers are used as asphalt modifiers which reduce viscosity at laying temperatures and improve cracking resistance, aging resistance, chemical compatibility, the strength of the mixture, and the stability at service temperature. Improvements with the polymer modifications depend on the polymer type, its dosage, and the quality of the vacuum residue.

Using RAP, RAS and Recycled Engine Oil Bottoms (REOB) as asphalt modifiers have been popular for decades. REOB is a waste stream obtained from the distillation of used motor oils, and is widely used in Canada and the United States as an asphalt additive due to its low cost and the fact that it has become more widely available in recent years [64]. RAP and RAS have been popular across the world for decades, and reduce the production cost of new asphalt mixtures by minimizing the virgin material requirements. RAP and RAS are most frequently used in Hot Mixed Asphalts production while RAP has become the major recycled material in the United States of America as recycling of asphalt pavement material is an economically and feasible process to rehabilitate old pavements. In addition to the economic benefits of using reclaimed asphalt materials, it also reduces the environmental footprint.

### 2.8.1 Polyethylene terephthalate (PET) as a Modifier

The PET is a thermoplastic polymer which is one of the most recycled polymers. It has high mechanical properties with excellent dimensional stability under varying loads. The polymer is transparent and widely used to produce drink containers, garments and magnetic tapes. Its resistance to impact, moisture, alcohols and solvents makes the bottle production accounting for about 30 % of global demand. Recycled PET can be easily converted to fibers which are highly flexible.

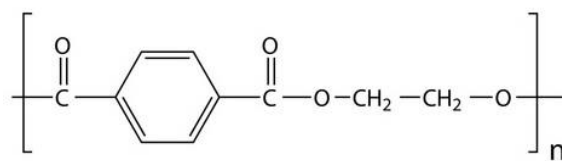


Figure 2.22: Molecular Structure of Polyethylene Terephthalate (PET).

Utilization of recycled PET fibers in asphalt mixtures can improve properties such as the softening point, resistance to rutting, durability, viscoelastic property and fatigue life [65].

Different methods were used to incorporate PET with an asphalt mixture. In the former process, the additives are mixed with the asphalt binder before being added to the mix, and

then, both are united with the aggregates later. In the latter process, the additive is combined with the aggregates before adding the asphalt binder [66].

### ***2.8.2 Reclaimed Asphalt Pavement as Asphalt Modifiers***

The asphalt binders in RAP and RAS are aged and highly oxidized due to its long service period. Maltenes in the asphalt structure convert to asphaltenes during the aging process, which decreases the maltenes/asphaltenes ratio. Hence, asphalt becomes stiffer and brittle. Aged asphalt pavements and roofing should be removed at the end of their lifetimes and replaced by new asphalt layers. As a result, a hundred million tons of RAP and RAS have been generated annually [67]. The RAP and other construction wastes have been acknowledged to be reused in road base layers, road shoulder, and rural road. Also, RAP and RAS can be added in the Hot Mixed Asphalt (HMA) surface layer of pavement with a certain percentage [68].

Ideally, the addition of RAP and RAS should not affect the performance of the virgin asphalt material. Hence, it is recommended to mix lower percentages (< 20 %) of RAP and RAS with the virgin material as the higher percentages might cause a negative impact of the asphalt mixture. However, using high rates of RAP and RAS positively impacts cost-saving and environmental footprint. The environmental and financial restrictions are forcing researchers to incorporate a high percentage of RAP and RAS in pavement construction. One of the main barriers to achieving this goal is the increased stiffness of the RAP and RAS binders [69]. The use of chemical additives referred to as rejuvenators or recycling agents has been pursued in recent years due to renewed interest in increasing the quantities of RAP and RAS in asphalt mixtures [70]. It is expected that the addition of rejuvenators decreases the stiffness of reclaimed asphalt materials and potentially improve cracking resistance of the asphalt mixture. But, some researchers are against using rejuvenators as the undesirable softening of asphalt with the addition of rejuvenators might negatively impact rutting resistance.

The following concerns are expressed on the utilization of RAP with modified and unmodified binders [71]:

- (i) Change in mixing and compaction temperatures
- (ii) Selection of base binder
- (iii) Temperature susceptibility
- (iv) Performance under different frequency, strain, and temperature
- (v) Rutting performance
- (vi) Fatigue performance, and
- (vii) Chemical changes

However, it is difficult to monitor and regulate the using of RAP and RAS as there is not enough information on how they affect the performance of neat asphalt and there is a lack of protocols to guide constructors on the amount of RAP and RAS that should be added to keep the desirable performance of the road.

### ***2.9 Chemical Compatibility of Modifiers***

The concept of binder compatibility or stability refers to the balance between soluble and insoluble fractions in the colloid, which controls the flow properties of the colloid [72]. A larger proportion of soluble fractions/maltenes results in a softer binder with increased ductility while a higher ratio of insoluble fraction/asphaltene in the asphalt structure results in a stiffer and more brittle binder. Reclaimed asphalt materials are more brittle as they contain a higher ratio of asphaltene, resulting from the oxidation.

When assessing the colloidal stability of asphalts, the main factor taken into account is the content of asphaltenes; consequently, the asphaltene index can be found suitable (equation 15) [73].

$$\text{Asphaltene Index (Ia)} = \frac{\text{Asphaltenes} + \text{Resins}}{\text{Saturates} + \text{Aromatics}} \quad (15)$$

The Gaestel instability index is another index to determine the asphalt stability, shows the dispersing capability of maltenes to asphaltenes (equation 16).

$$\text{Gaestel Index (Ic)} = \frac{\text{Saturates} + \text{Asphaltenes}}{\text{Resins} + \text{Aromatics}} \quad (16)$$

Colloidal stability of asphalt decreases with increasing the Gaestel index value. Both indexes are high when an asphalt binder has higher asphaltene content. Recycling heavily aged asphalt binders into new asphalt pavements while maintaining sufficient durability is challenging, as recycled binders have a larger asphaltene content as compared to new paving binders and are therefore significantly stiffer and more brittle [74]. Target performance grades of the asphalt blend might be achieved by mixing softer (asphalt which contains low asphaltene content) virgin asphalt with reclaimed asphalt material.

## ***Chapter 3***

### ***Materials and Experimental Methods***

#### ***3.1 Materials***

Neat asphalts used in this project were obtained from Alberta oil sands where the asphalt binder represented as C is from a Cold Lake deposit, the neat asphalt called A was obtained from an Athabasca deposit, the P binder was provided from a Peace River deposit, and B neat asphalt was obtained from a conventional oil production in Alberta. The two RAP samples were supplied by the Ministry of Transportation of Ontario from Highway 7 in central Ontario and Highway 403 in the Greater Toronto Area (GTA). Highway 7 is around 25 years old which is still in a good shape while Highway 403 is about 5 years old which has an excessive amount of premature cracking in its structure. Reclaimed asphalt shingles were provided from a tear-off shingles sourced from a local contractor. Additional RAP for HMA tests was provided from a local hot mix plant in Kingston, Ontario.

#### ***3.2 Recovery of Reclaimed Asphalt Binder***

Sufficient amounts of RAP and RAS were soaked in three clean covered paint cans with dichloromethylene (DCM) overnight and washed several times with solvent to ensure as much as possible of the asphalt binder was removed by the solvent. Next, the dissolved asphalt in DCM was run twice through a high-speed centrifuge to remove the fines in the solution and the extractions were collected into three separate clean bottles labeled as 7, 403 and RAS.

Binders were recovered by using the Buchi R-210 Rotavapor system under a dry nitrogen atmosphere. To recover the binders, a condensation temperature between 50 °C and 80 °C was used with an aspirator pressure of 450 mbar. Once most of the solvent was evaporated, the temperature was increased up to 160 °C in 20 °C incremental steps. Once the disappearance of condensed solvent dropping out, the system was kept under pressure below 100 mbar and 160 °C for an hour to ensure there are no more traces remain in the recovered

asphalt binder. Then, recovered asphalt binders were transferred to clean beakers for further testing.

### **3.3 Modification of Neat Binders**

Neat asphalt binders were modified at two different weight percentages (20 % and 40 %) by mixing recovered RAP and RAS with neat asphalts. For instance, to have the C + 20 % Hwy 7 blend, 20 g of recovered Hwy 7 RAP was added to a clean labeled beaker. Then, 80 g of neat C was added to the same beaker in order to obtain a total weight of 100 g. The blend was melted and mixed well to have a homogeneous asphalt blend of C and 20 % Hwy 7 recovered binder. A total of 12 different blends were used and the above procedure was followed to obtain each blend. Obtained blends are listed in Table 3.1.

*Table 3.1: Prepared asphalt binder blends.*

<b>Modified C Blends</b>	<b>Modified A Blends</b>
C + 20 % Hwy 7	A + 20 % Hwy 7
C + 40 % Hwy 7	A + 40 % Hwy 7
C + 20 % Hwy 403	A + 20 % Hwy 403
C + 40 % Hwy 403	A + 40 % Hwy 403
C + 20 % RAS	A + 20 % RAS
C + 40 % RAS	A + 40 % RAS

### **3.4 Aging of Asphalt Binder**

In the laboratory, the short term aging that occurs during mixing and compaction of hot mixed asphalts is simulated by the RTFO method according to ASTM standard D 2872-97 and the long term aging that occurs in service is simulated using the PAV method in accordance to ASTM D 6521-13 or AASHTO R 28-06.

#### **3.4.1 Short-Term Aging**

Solid asphalt samples were melted in the oven (160 °C) for 15 min to pour samples into RTFO tubes. A weight of 35 g of the samples were poured into the clear labeled RTFO tubes

and kept horizontally in the racks for an hour to condition at room temperature. After the conditioning, tubes with the samples (8 tubes per one time) were placed in the Rolling thin-film oven and rotated at 15 rpm for 85 min at 163 °C (see Figure 3.1). Airflow into the tubes was maintained at 4000 mL/min during the short term aging period.



*Figure 3.1: RTFO aging. A) Loading the glass tube, b) Rolling in RTFO and c) coated tube after aging [75].*

### **3.4.2 Long-Term Aging**

A total of 6.4 g of RTFO aged sample was poured into a 50 mm stainless steel PAV tin to obtain a 3.2 mm thickness of the asphalt binder layer. Two PAV plates with the binder were prepared for each sample (2 neat binders and 12 blends) according to the above procedure. Then, plates were arranged in the PAV rack and placed inside the PAV. Next, the PAV was covered tightly to prevent leakage of air pressure and temperature. Samples were aged for 20 h under 2.08 MPa pressure and 100 °C temperature.

After 20 h, one plate from each sample was taken out and the rest of the samples were aged for another 20 h by using the same conditions. Eventually, there were two batches of the same samples which were 20 h aged and 40 h aged.

### **3.5 Dynamic Shear Rheometer**

DSR frequency sweep tests were performed on all the samples to evaluate the binder resistance to rutting and fatigue cracking at intermediate and high temperatures. All tests were conducted using Discovery Hybrid 1 (DHR-1) and Discovery Hybrid 2 (DHR-2) TA Instruments.

For the intermediate temperature frequency sweep DSR tests, melted asphalt binder was poured into a silicon-mold in order to take a thin asphalt layer around 8 mm diameter. Next, the asphalt binder thin layer was loaded into a pre-calibrated DSR instrument which has an 8 mm parallel plate configuration (a lower fixed plate and an upper movable plate). The loading temperature was 64 °C and the loading gap was set to 2.1 mm. The sample was kept around 10 min at 64 °C and then the samples were trimmed around the edges of the plate using a trimming tool. Then, the gap was reduced to 2 mm to have the testing gap and conducted testing at 34 °C, 22 °C, 10 °C and -2 °C temperatures at 0.1 to 10 rad/s frequency range and adequately selected torque and strain values.

For the high-temperature frequency sweep DSR tests, around 25 mm thin asphalt layer was obtained by pouring melted asphalt into the respective silicon mold. The loading gap of the 25 mm parallel plate configuration was 1.1 mm and the loading temperature was 64 °C. Samples around the edges of plates were trimmed after keeping the sample around 10 min at 64 °C. Here, 1.0 mm used as the testing gap and conducted testing at 70 °C, 58 °C, 46 °C and 34 °C temperatures at 0.1 to 10 rad/s frequency range and adequately selected torque and strain values. Two trials for each DSR test were done and the repeatability of test results was within  $\pm 1$ .

### ***3.6 Fourier-Transform Infrared (FTIR) Spectroscopy***

FTIR method is one of the best analytical methods and most used technique to analyze chemical changes of asphalt with the oxidative aging while RTFO aging and PAV aging. In this project, a Perkin-Elmer Spectrum™ 400 FTIR spectrometer was used to analyze the functional groups and proportion of functional groups present in all unaged, RTFO, PAV-20 h and PAV-40 h aged binders. Functional groups and respective wavenumber ranges are in Table 3.2.

Table 3.2: Wavenumber ranges of functional groups.

<b>Functional Groups</b>	<b>Wavenumber range</b>
Styrene	710 cm <sup>-1</sup> – 696 cm <sup>-1</sup>
Butadiene	983 cm <sup>-1</sup> – 955 cm <sup>-1</sup>
Sulfoxides	1070 cm <sup>-1</sup> – 985 cm <sup>-1</sup>
CH <sub>3</sub>	1400 cm <sup>-1</sup> – 1300 cm <sup>-1</sup>
Aromatics	1650 cm <sup>-1</sup> – 1535 cm <sup>-1</sup>
Carbonyl	1760 cm <sup>-1</sup> – 1655cm <sup>-1</sup>
CH <sub>2</sub>	3121 cm <sup>-1</sup> – 2746 cm <sup>-1</sup>

The CH<sub>2</sub> group was used as the internal standard as it is oxidation resistant compared to the other groups. The index of the individual functional groups was determined by taking the ratio of the specific functional group peak area to that of the CH<sub>2</sub> peak area. The IR absorption by a sample depends on IR wave path length (l), concentration (c) of functional group and molar extinction coefficient ( $\epsilon$ ) where  $\epsilon$  depends on the functional group.

A KBr pellet was pre-heated for 3 minutes at 140 °C and a small amount of sample was smeared on top of the KBr pellet to have a thin film of the sample. After performing the background test which was controlled by the FTIR software, the KBr pellet with the dry asphalt film was placed in the sample holder in the spectrometer. Then, 16 scans were carried out over the wavenumber range of 4000 cm<sup>-1</sup> to 400 cm<sup>-1</sup> by using FTIR software.

### 3.7 Hot Mixed Asphalt (HMA).

The following quantities were used to prepare HMA specimens for further testing. All quantities are for two bricks with 150 mm diameter and 50 mm height.

Table 3.3: Components of HMA

<b>Component</b>	<b>Weight, g</b>	<b>Percentage, %</b>
Asphalt binder	221.17	4.90
Course aggregate (12.5mm)	1545.30	34.24

Fine aggregate (9.5mm)	343.40	7.61
Main sand	2403.75	53.26

Total weight = 4513.62 g

All mixing equipment and components were kept at 160 °C for 1 hour and mixed all together until to have well-mixed asphalt concrete HMA. It is important to mix all components under hot conditions. Hence, it is advisable to do mixing quickly while components are at high temperatures (mixed before cool down).

Then the HMA was transferred into two cans, 2051.63 g for each. That was the weight used to prepare one brick of Asphalt Concrete (AC). Cans were sealed and kept at 140 °C for 16 hours before the compacting. In the test, one type of HMA had 4 cans, two belong to room temperature tests and the other two belong to -10 °C temperature tests.

To have the RAP modified HMA, 221.17 g of asphalt binder blend was prepared by adding 20 % of RAP (44.23 g) and 80 % (176.94 g) of virgin asphalt binder. To have the PET modified HMA, 13.64 g of PET fibers were added to the HMA while mixing it. It is about 0.30 % of the total weight of the HMA (4513.62 g).

### ***3.7.1 Preparation of Test Specimens.***

A total of 2051.63 g of HMA was transferred into the mould and compacted using the gyratory compactor (see Figure 3.2). A cylindrical disc of HMA with smooth parallel surfaces was obtained (4 cylindrical discs were obtained for one type of HMA). The diameter of the disc was  $150 \pm 1$  mm and the height was  $50 \pm 1$  mm. Compacting pressure was 600 KPa, the gyration was 704 and the angle was  $1.16^\circ$ .



*Figure 3.2: Pine Instruments gyratory compactor.*

Each cylindrical disc was cut exactly in half to produce two identical, semi-circular Illinois Flexibility Index Test (I-FIT) specimens (see Figure 3.3). Each slice had parallel, smooth faces. Then, a notch was cut along the axis of symmetry of each individual I-FIT specimen to a depth of  $15 \pm 1$  mm and  $1.5 \pm 0.1$  mm in width.

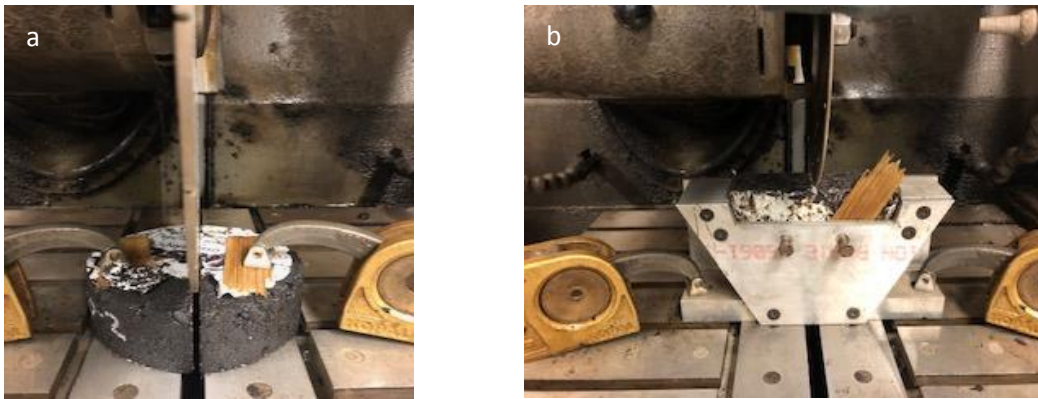


*Figure 3.3: Cutting the specimen a) into halves, b) notch along the axis.*

### **3.7.2 Illinois Flexibility Index Test (I-FIT)**

The Material Test Systems MTS 810 servo-hydraulic test frame was used to conduct I-FIT test. The test specimen was positioned in the test fixture on the rollers so that it is centered in both the “x” and the “y” directions and so that the vertical axis of loading is aligned to pass from the center of the top radius of the specimen through the middle of the notch (see Figure 3.4) [61]. First, imposed a small contact load of  $0.1 \pm 0.01$  kN in stroke control with a loading rate of 0.05 kN/s. Axial displacement with the force was obtained throughout the test. The test was stopped when the load drops below 0.1 kN. Specimens were tested under two temperatures,

room temperature and -10 °C. Specimens were kept at -10 °C for 2 h before conducting lower temperature (-10 °C) tests.



*Figure 3.4: Illinois Flexibility Index Test*

Load vs. axial displacement curves were plotted for each specimen. For each test, four I-FIT specimens were available from one type of HMA. A minimum of three individual I-FIT specimens was defined as one I-FIT test.

## *Chapter 4*

### *Results and Discussion*

#### *4.1 Dynamic Shear Rheometer Results*

The DSR instrument was used to measure the complex shear modulus  $G^*$  and the phase angle  $\delta$  which relate to the elastic response and the viscous response from the unaged, RTFO, and PAV samples. This provides a measure of stiffness and relaxation ability of the binder. These results are used to evaluate the effect of adding RAP and RAS into the virgin asphalt binders and evaluate the changes of rheological properties of asphalt with aging. Further, these results give a good indication of how neat asphalt binder softness affects the accommodation of RAP and RAS materials.

##### *4.1.1 High Temperature Performance Grade (HTPG)*

HTPG is used to evaluate the rutting resistance of the binder, which also gives a good projection on binder softness. It is known that more brittle binders have high HTPG and this ultimately reduces the binder's susceptibility to rutting. Softer binders have low HTPG and which ultimately increases the susceptibility to rutting. The HTPG of the samples was determined using the rutting resistance factor  $G^*/\sin\delta$  at  $G^*/\sin\delta > 1.00$  kPa for unaged samples and  $G^*/\sin\delta > 2.20$  kPa for RTFO-aged samples [56]. The following table contains the HTPG of two neat asphalt binders, C and A.

*Table 4.1: HTPGs of two base asphalt samples*

<i>Base Asphalt</i>	<i>HTPG, °C</i>
C	61
A	54

It can be seen that A has a lower HTPG than C and the difference is 7.60 °C, which a little more than a full grade. Hence, A neat binder should be considerably softer than C. As harder asphalts contain high asphaltene contents, C must contain higher asphaltene percentage

than A. Binder C should therefore also possess higher rutting resistance compared to A. However, it is known that both neat binders perform well in-service if the aggregate design is rut resistant.

The following graphs (Figure 4.1) show the changes of HTPG of base asphalts with the addition of RAP and RAS.

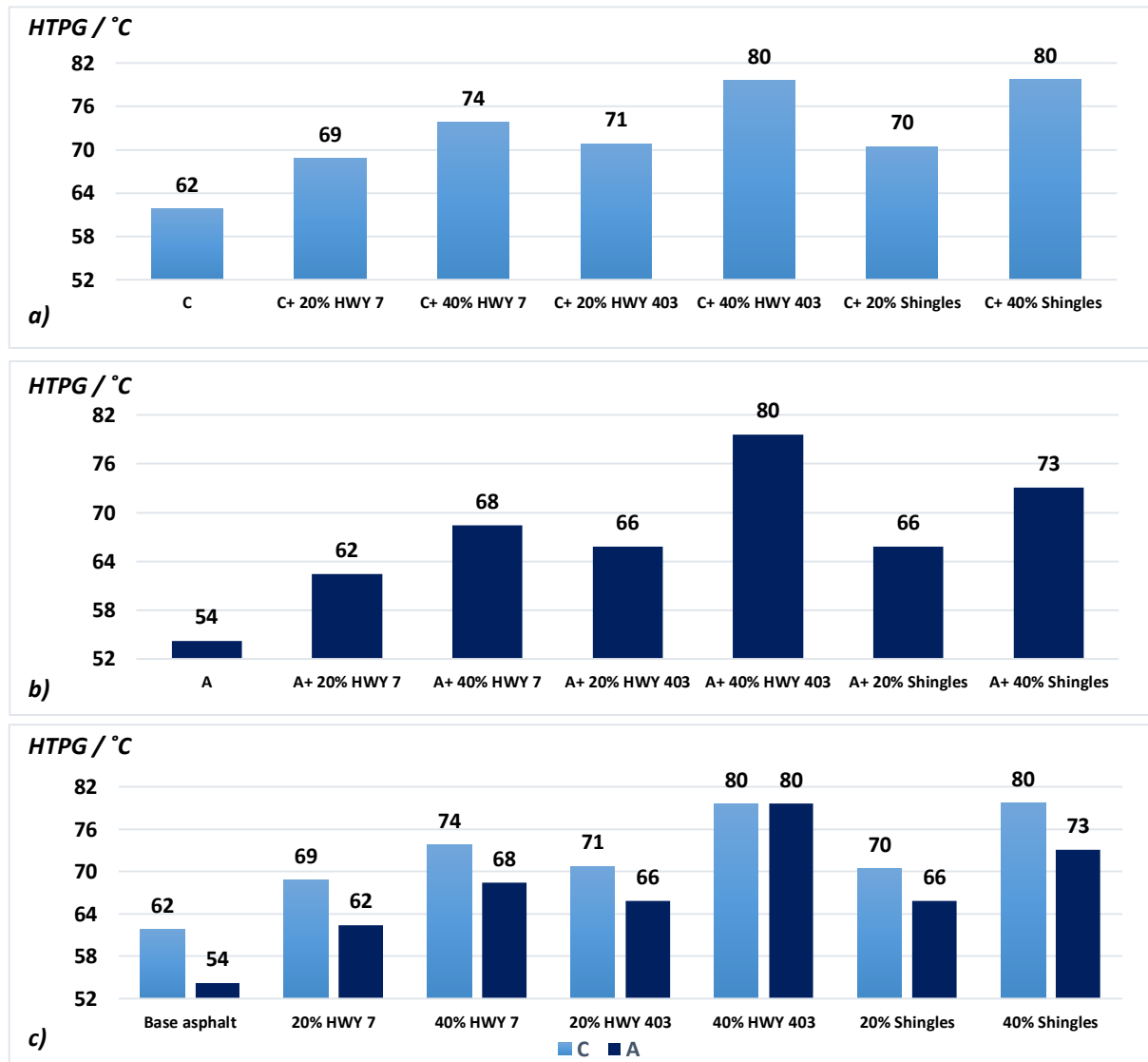


Figure 4.1: Changes of HTPG with addition of RAP and RAS into base asphalts. a) HTPG of C asphalt blends, b) HTPG of A asphalt blends and c) Comparison of HTPGs of C based asphalt blends and A based asphalt blends.

According to the graph (a) and (b), the HTPG is increasing with adding RAP and RAS into the base asphalt. RAP and RAS have undergone oxidation and which has higher asphaltene

content in the asphalt colloidal structure. Thus, the addition of RAP and RAS into the base asphalt causes the increase of asphaltene content in the total asphalt blend and which results in a more brittle asphalt blend than base asphalt. This affects positively the rutting resistance of the binder. On the other hand, higher brittleness of asphalt blends negatively affects the fatigue and low-temperature performance of the binder. Brittle binders or binders with high HTPG are susceptible to fatigue and low temperature cracking.

The difference of the HTPG of the blend with the base asphalt has increased with the increasing RAP and RAS percentages. HTPG increases with the addition of 40 % Hwy 403 and 40% shingles into base asphalts are considerably higher than the addition of 40% Hwy 7 into base asphalts. It shows that Hwy 403 and RAS must contain higher asphaltene content in their colloidal structure than in Hwy 7. Shingles are aging faster than the asphalt pavement layer as roofs have thinner asphalt layers than pavement layers. Hence, roofing asphalt materials are susceptible to oxidation faster.

When considering the graph (c), in almost all the cases, the HTPG of C-based asphalt blends are higher than the corresponding A-based asphalt blends. This should be due to the initial brittleness of the C base asphalt compared to the A base asphalt. Hence, the total asphaltene content of the C based asphalt blends should be higher than the total asphaltene content of the A based asphalt blends. When an asphalt blend has a high asphaltene percentage, it increases both the Asphaltene and Geastel indexes (Equations 13 and 14 respectively) of the colloidal structure of the blend. Therefore, both indexes should be higher in C based asphalt blends. Colloidal stability of the asphalt structure decreases with increasing asphaltene and Geastel indexes. Hence, A based asphalt blends should have higher colloidal stability than C based asphalt blends. This shows that A base asphalt/ softer asphalt can accommodate a higher RAP and RAS percentage than in more brittle C base asphalt.

The HTPG of base C is relatively closer to the HTPG of A+ 20% Hwy 7 blend, A + 20% Hwy 403 blend and A + 20% RAS blend. This shows that the high temperature performance of the base C and A based blends with 20 % reclaimed asphalt materials may be similar to each other. It is advisable to add 20 % of reclaimed asphalt materials to A base asphalt to achieve comparable rutting resistance as the well performed C base binder.

#### ***4.1.2 Limiting Phase Angle Temperatures***

Phase angle values of asphalt samples obtained from DSR data are sensitive to the asphalt cement quality. Under high temperatures and low frequencies, the asphalt binder has a relatively high phase angle as it has fluid-like properties under the condition. At low temperatures and high frequencies, asphalt shows lower phase angle value as asphalt acts like an elastic solid. Hence, the phase angle of the asphalt binder decreases with increased stiffness.

It is found that limiting phase temperatures at phase angle  $45^\circ$  and  $27^\circ$  ( $27^\circ$  has been rounded to  $30^\circ$ ) are good crossover points to determine asphalt sample performances. At the point that the phase angle of the sample equals to  $45^\circ$ , the elastic modulus ( $G'$ ) and the viscous modulus ( $G''$ ) become equal, which indicates the equal contribution of elastic and viscous components of  $G^*$ . Consequently, the limiting temperature at phase angle  $45^\circ$  ( $T_{\delta=45^\circ}$ ) represents a balance between  $G'$  and  $G''$  and a transition from a more solid-like to a more fluid-like viscoelastic behavior [65]. Asphalt pavements operate in a wide temperature range, and when the pavement is above  $T_{\delta=45^\circ}$ , the binder will be more likely to flow under stress instead of cracking due to the predominant influence of the  $G''$  component [65]. The increasing of the  $T_{\delta=45^\circ}$  reduces the likelihood that the pavement temperature will be above  $T_{\delta=45^\circ}$ . Hence, asphalt samples with lower  $T_{\delta=45^\circ}$  have greater resistance to fatigue and thermal cracking as it can relax the stress. Asphalt samples with high  $T_{\delta=45^\circ}$  are stiffer and susceptibility to crack under stress.

Limiting temperature at phase angle  $27^\circ$ - $30^\circ$  ( $T_{\delta=30^\circ}$ ) is equally important as typical binders that are used in northern climates such as North America and northern Europe reach its

phase angle around  $27^\circ$  at  $0^\circ\text{C}$ . Thus this is a good parameter to rank binder cracking performances. The point is called the freeze-thaw point and, at this point, pavements undergo lots of movements as water freezes under the pavement layer at night time and it melts back in the day time, which results in lots of damage to the road surface. Stiffer asphalt binders have high  $T_{\delta=30^\circ}$ , which means that the binder phase angle becomes  $30^\circ$  at high temperatures, and these binders susceptible to cracking as it fails to relax the stress. Binders with low  $T_{\delta=30^\circ}$  can relax the stress and more resistance to cracking, those binders are softer and show fluid-like behavior even in relatively low temperatures.

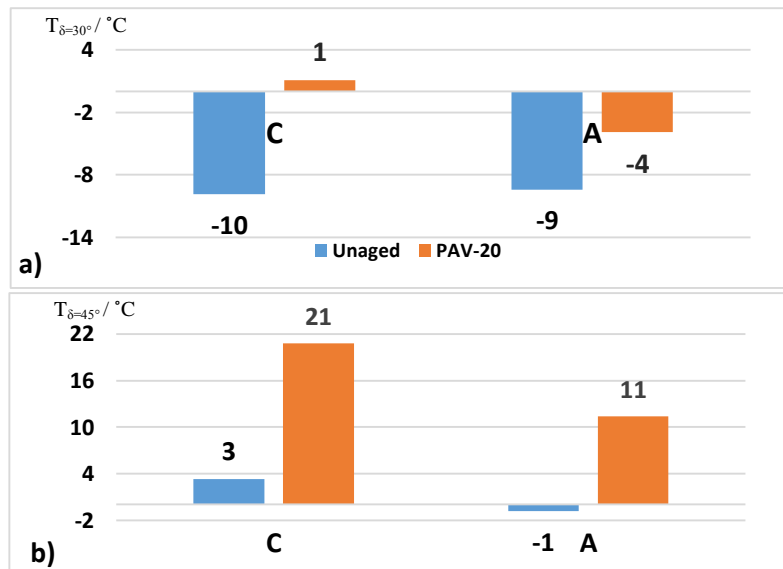


Figure 4.2: Limiting phase angle temperatures of two base asphalts at unaged and PAV-20 hours aging conditions, a)  $T_{\delta=30^\circ}$  and b)  $T_{\delta=45^\circ}$

Both limiting phase angle temperatures are higher in PAV-20 h condition as binders become stiffer and brittle with the aging (see Figure 4.2). This should be due the conversion of maltenes into asphaltene with the oxidation of binders.

There is no significant difference of  $T_{\delta=30^\circ}$  in the two unaged base asphalt binders, but after aging for 20 h in the pressure aging vessel, the  $T_{\delta=30^\circ}$  different is about  $5.0^\circ\text{C}$  where the A value is negative and the C value are slightly higher than  $+1^\circ\text{C}$ . The  $T_{\delta=45^\circ}$  difference between the two base asphalt is about  $4.2^\circ\text{C}$  when it is in the unaged condition and the

difference is significantly bigger after the aging (9.4 °C). Overall, both  $T_{\delta=30^\circ}$  and  $T_{\delta=45^\circ}$  are smaller in the A base asphalt binder than in the C base asphalt binder. Results show that A base binder can relax the stress more efficiently and it should have a higher resistance to fatigue and thermal cracking. The softness of the asphalt results in more fluid-like properties in intermediate and low temperatures than in stiffer binders.

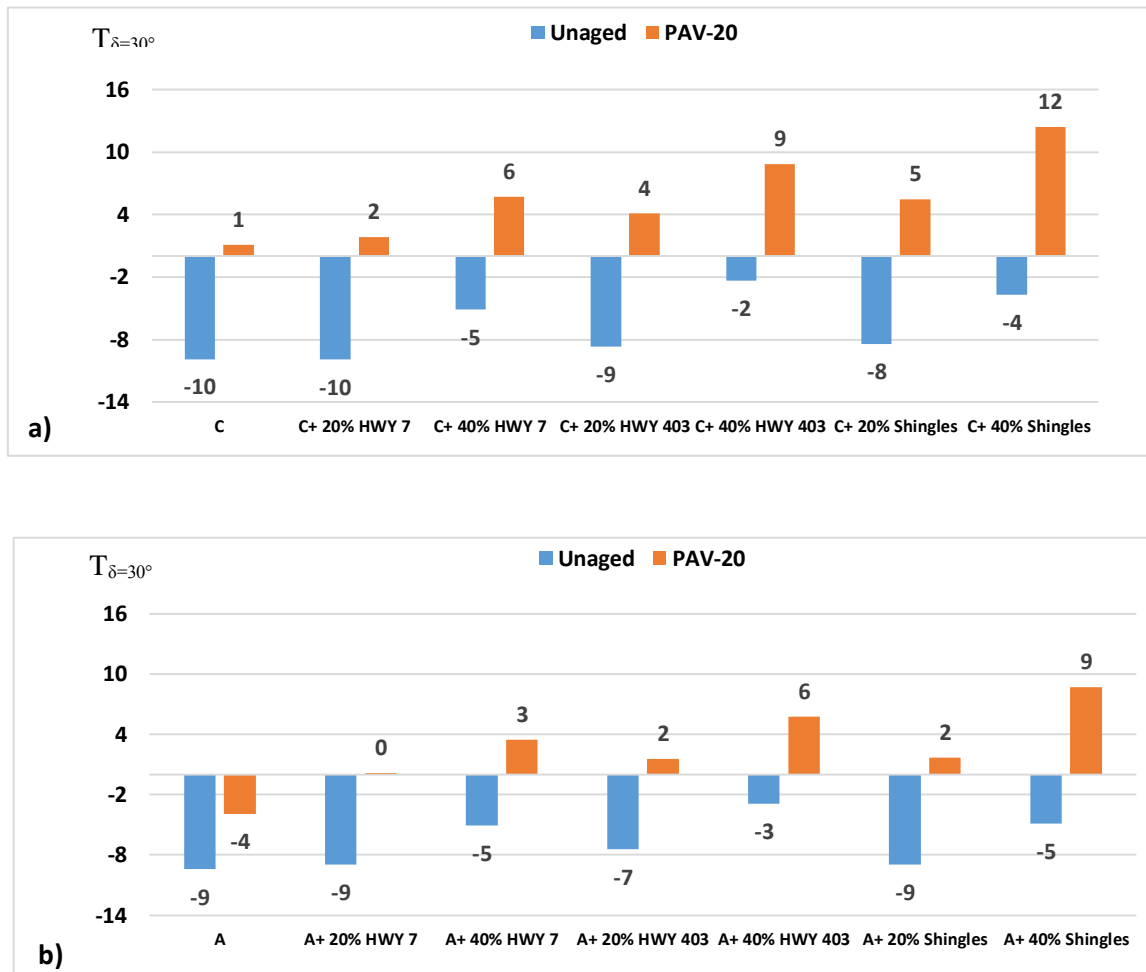


Figure 4.3:  $T_{\delta=30^\circ}$  of asphalt blends at unaged and PAV-20 h aging conditions, a) C based asphalt blends and b) A based asphalt blends.

$T_{\delta=30^\circ}$  values of the two base asphalts are increasing with the addition of reclaimed asphalt materials and the values increase with the rising of the RAP ratio in asphalt blends (see Figure 4.3).

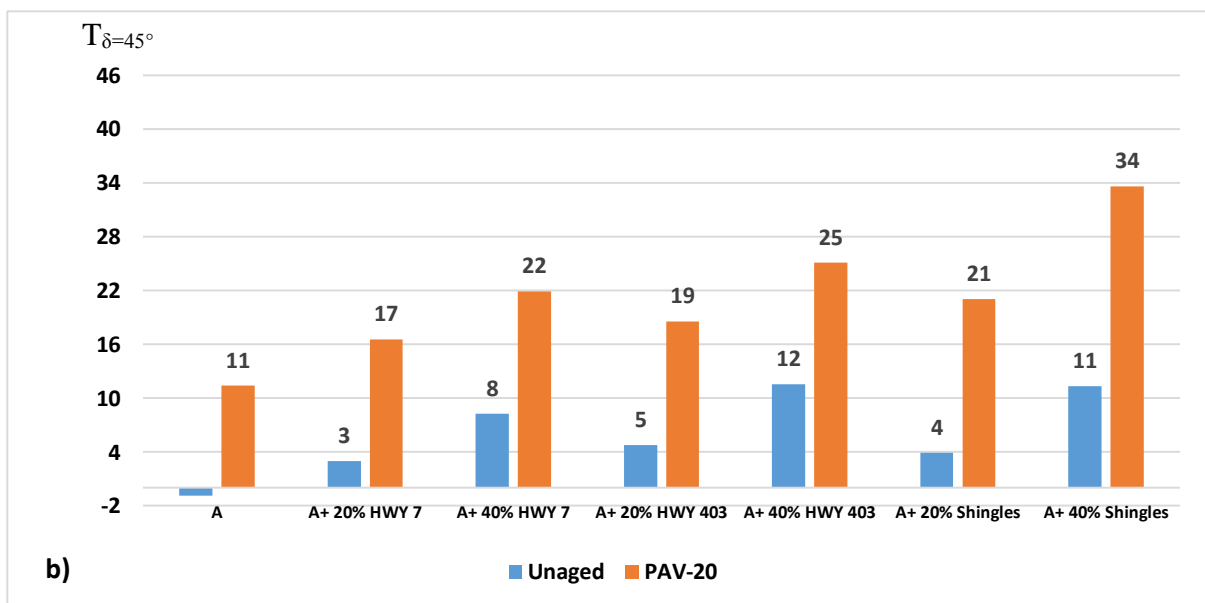
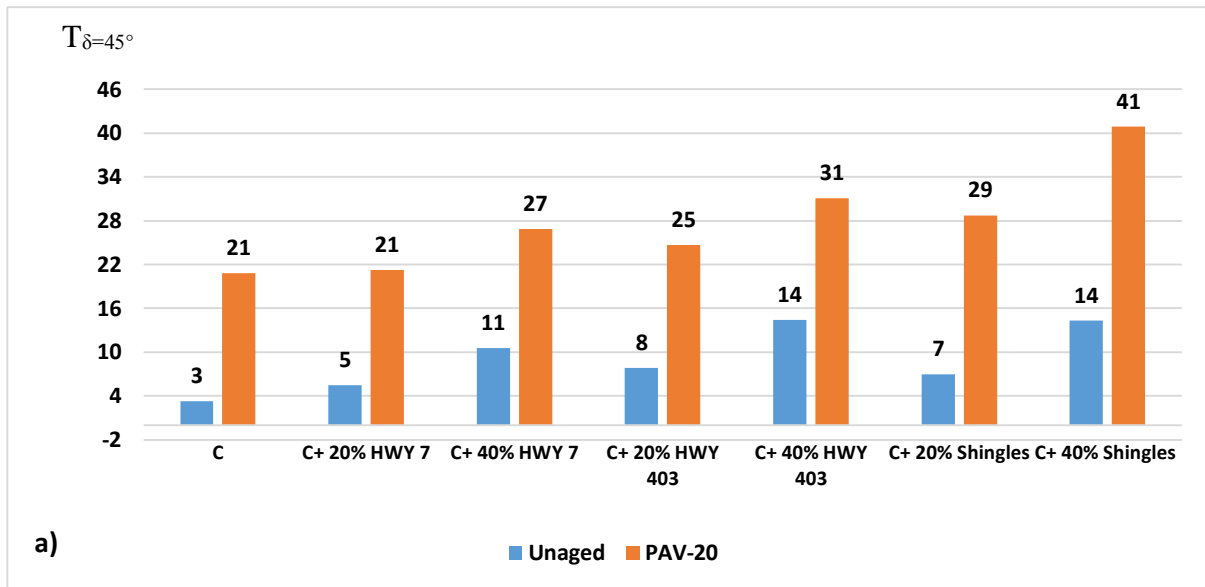


Figure 4.4:  $T_{\delta=45^\circ}$  of asphalt blends at unaged and PAV-20 h aged conditions, a) C-based asphalt blends and b) A-based asphalt blends.

The increases of both  $T_{\delta=30^\circ}$  and  $T_{\delta=45^\circ}$  with the aging should be due to the oxidation of maltenes in the asphalt structure. Oxidation converts maltenes into asphaltenes, which increases the stiffness of the asphalt structure. Addition of RAP and RAS affects both  $T_{\delta=30^\circ}$  and  $T_{\delta=45^\circ}$  values of base asphalt as a result of the increase of the stiffness of the base binder

along with the RAP and RAS addition. The increase of the  $T_{\delta=45^\circ}$  with the aging and RAP and RAS addition is significantly higher than the increase of the  $T_{\delta=30^\circ}$ .

According to figure 4.3,  $T_{\delta=30^\circ}$  values of the corresponding C-based asphalt blend and A-based asphalt blend do not show a significant difference when they are in the unaged condition. For instance,  $T_{\delta=30^\circ}$  values of unaged C + 20 % Hwy 7 blend and A + 20 % Hwy 7 blend are relatively closer to each other. The same trend can be seen in other corresponding blends as well (C-based blends and A-based blends). However,  $T_{\delta=30^\circ}$  values of C-based asphalt blends are significantly larger than the corresponding A-based asphalt blends, after the aging for 20 h in the pressure aging vessel. As an example, the  $T_{\delta=30^\circ}$  value of the PAV-20 h aged C + 20 % Hwy 7 is 1.82 °C and the value is 0.15 °C in PAV-20 hrs aged A + 20 % Hwy 7 blend, such that the variance is more than 1.5 °C.

According to figure 4.4,  $T_{\delta=45^\circ}$  values are higher in C-based blends than A-based blends. This should be due to the initial stiffness of the C-based binder where A-based binder is softer than the C-based binder. Results indicate that the initial stiffness of the base binder affects the low- and intermediate-temperature performance of the asphalt blend.

Both  $T_{\delta=30^\circ}$  and  $T_{\delta=45^\circ}$  increase with increasing of RAP and RAS ratio in the blend. This shows that asphalt binder blends performances depend on the RAP and RAS ratio. The high RAP and RAS ratio results in a stiffer blend and which negatively affects the low- and intermediate-temperature performances of the binder blends. Further, the addition of reclaimed Hwy 403 and RAS into both base asphalt result a higher increment in limiting phase angle temperatures than besides of reclaimed Hwy 7 into base asphalts. For instance,  $T_{\delta=45^\circ}$  in PAV-20 h aged C + 20 % Hwy 7 blend is 21.24 °C and the same limiting phase angle temperature in PAV-20 h aged C + 20 % RAS is 28.71, such that the difference is more than 7 °C. Hence, the quality of the reclaimed material significantly affects the low and intermediate temperature performances of the asphalt blend. The quality of the reclaimed Hwy 7 sample should be better

than the quality of Hwy 403 and RAS. The quality of reclaim materials depends on the oxidation level/aging level of the sample.

Although the addition of 20 % RAP and RAS into the base C results in a significantly higher  $T_{\delta=45^\circ}$  values than the  $T_{\delta=45^\circ}$  of base C, the  $T_{\delta=45^\circ}$  values of A + 20 % RAP and RAS blends are closer to the  $T_{\delta=45^\circ}$  value of well performed base C asphalt, as shown in Figures 4.5 and 4.6.

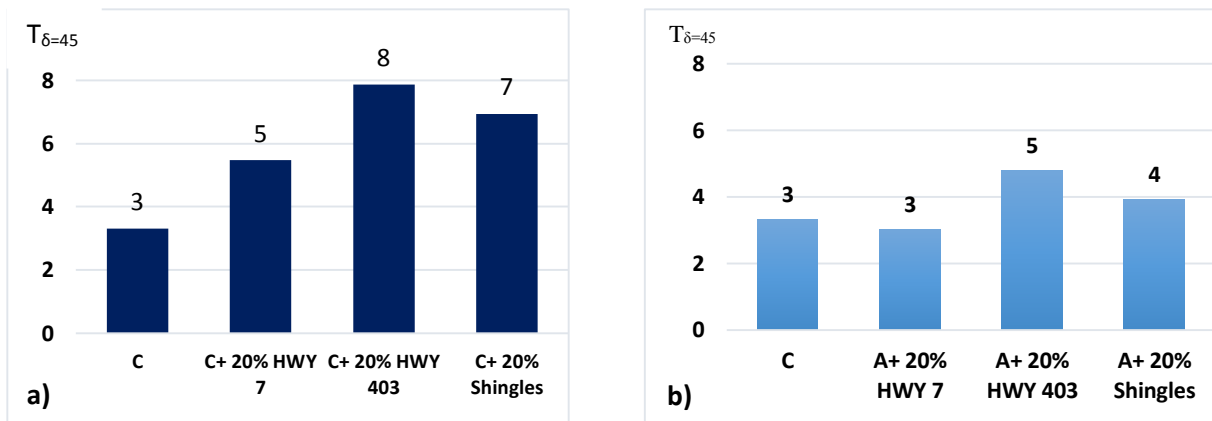


Figure 4.5:  $T_{\delta=45^\circ}$  comparison with base C binder (unaged condition). a) 20 % RAP and RAS with base C and b) 20 % RAP and RAS with base A.

The  $T_{\delta=45^\circ}$  value of A + 20 % Hwy 7 is 3.01 °C, which is slightly lower than the  $T_{\delta=45^\circ}$  value of base C. Also, there are no significant variances of the  $T_{\delta=45^\circ}$  of A+ 20 % Hwy 403 and A + 20 % RAS with the base C binder. Hence, the low and intermediate temperature performances of A based 20 % RAP and RAS blends may be similar to the performances of base C. Graph 4 shows that the  $T_{\delta=45^\circ}$  comparison of 20 % RAP and RAS blends with the base C in PAV-20 h aged condition.

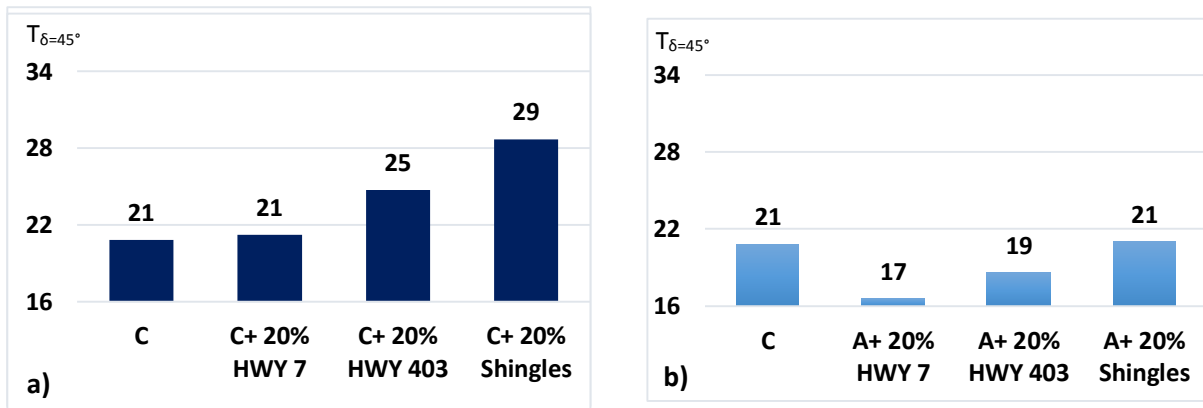


Figure 4.6:  $T_{\delta=45^\circ}$  comparison with base C binder (PAV-20 hours aging condition). a) 20% RAP and RAS with base C and b) 20% RAP and RAS with base A.

After the aging, the  $T_{\delta=45^\circ}$  value of A+ 20 % Hwy 7 blend is lower than the base C and the difference is around 4 °C. Also, there is a 2 °C difference of  $T_{\delta=45^\circ}$  values between base C and A + 20 % Hwy 403 blend where the  $T_{\delta=45^\circ}$  value of the A + 20 % Hwy 403 blend is lower. The low and intermediate temperature performance of A + 20 % of RAP blends may be better than the performance of base C.

The following figures (4.7 and 4.8) show that the comparison of  $T_{\delta=30^\circ}$  of 20 % RAP and RAS blends with the base C in both unaged and PAV-20 h aging conditions.

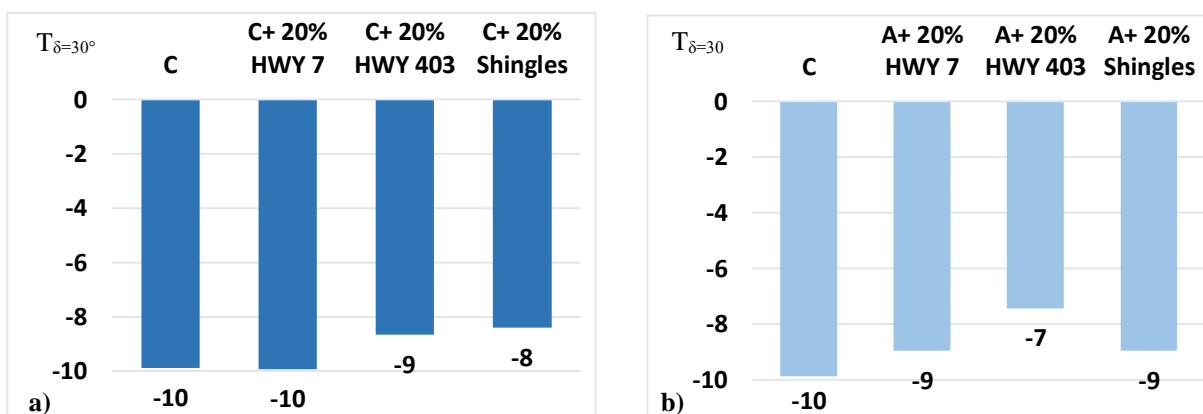


Figure 4.7:  $T_{\delta=30^\circ}$  comparison with base C binder (unaged condition). a) 20 % RAP and RAS with base C and b) 20 % RAP and RAS with base A.

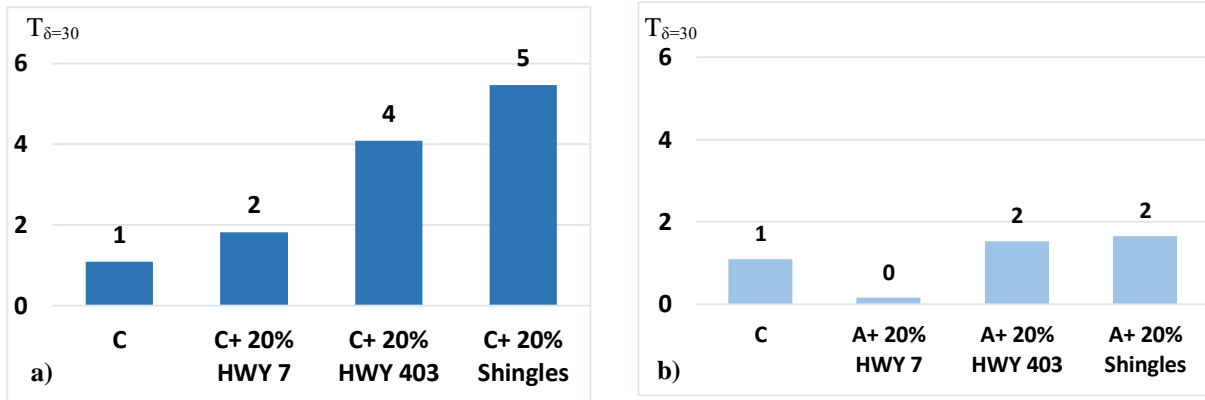


Figure 4.8:  $T_{\delta=30}$  comparison with base C binder (PAV-20 h aging condition). a) 20 % RAP and RAS with base C and b) 20 % RAP and RAS with base A.

The addition of 20 % RAP and RAS into base asphalt does not significantly affect to the  $T_{\delta=30}$  before the aging. However, after aging for 20 hours in PAV, the  $T_{\delta=30}$  difference is significant between base C based 20 % RAP and RAS.  $T_{\delta=30}$  of A based 20% RAP and RAS and base C is relatively closer at the PAV-20 h aged condition.

#### 4.1.3 Grade Span

According to the Superpave specification, the higher the grade span the better the performance of the asphalt cement. In this experiment, grade span was used to determine the changes of asphalt binders with the modifications, distinguish the lesser quality modified asphalts from the superior quality materials, and to compare performance similarities between the modified A base blends and the C base asphalt.

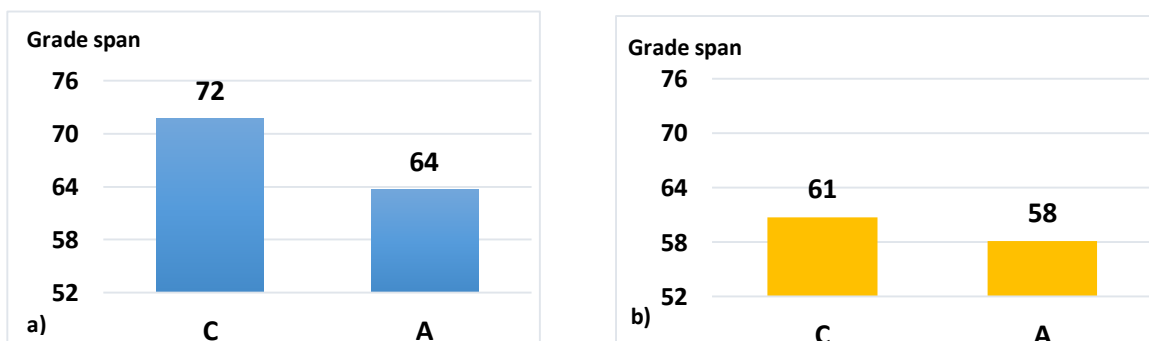


Figure 4.9: Grade span of two neat asphalts a) Unaged conditions b) PAV-20 h aging condition.

In both cases, A has a lower grade span than the C (see Figure 4.9). Whether A has a lower grade span than the C, A is known as a well performed neat binder. After the 20 h aging, the grade span of the neat C has reduced by 10.98 while A has reduced by 5.53. This shows that the aging affects the grade span of neat C more than the grade span of neat A.

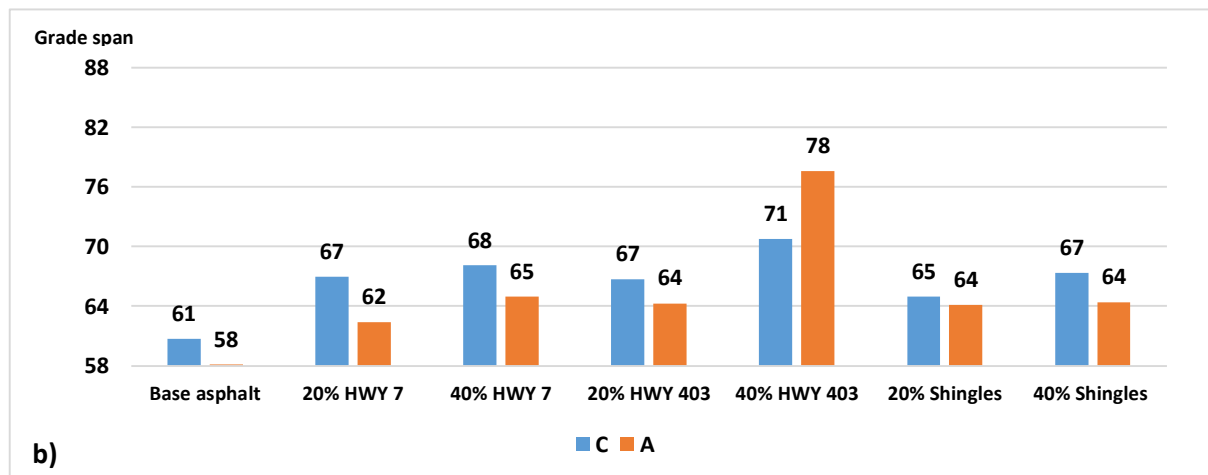
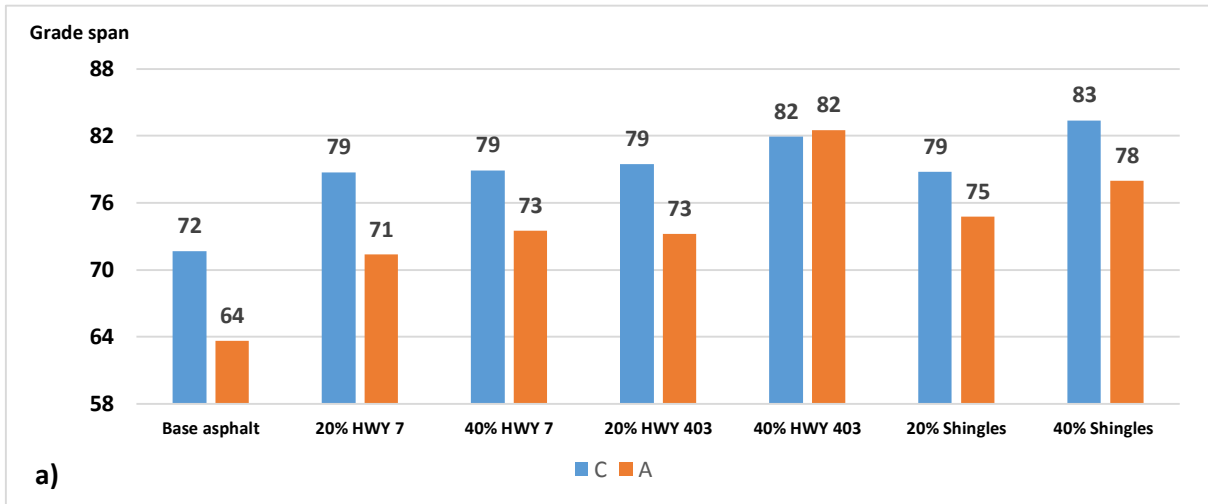


Figure 4.10: Grade spans for asphalt binder blends included C and A base asphalts (a) unaged samples (b) PAV-20 h aged samples.

The grade span has increased with the addition of RAP and RAS into base binders and the grade span is higher in blends with high RAP and RAS percentages (see Figure 4.10). This may be due to the increase in the high temperature performance with the high asphaltene content in the asphalt blends. The addition of 40 % RAP and RAS into neat asphalt results in

a high difference of grade span between the base binder and the modified asphalt blend. In all cases, the grade span has decreased with aging.

Addition of 40 % Hwy 403 and 40 % RAS into base asphalts results in a drastic increase in the grade span. The addition of 40 % Hwy 7 does not considerably affect the grade span of base asphalt. This indicates that asphalt modification with reclaimed Hwy 7 gives higher modified blends than the modification with reclaimed Hwy 403 and RAS. The following graphs shows that comparison of grade span values of base C and A + RAP and RAS blends.

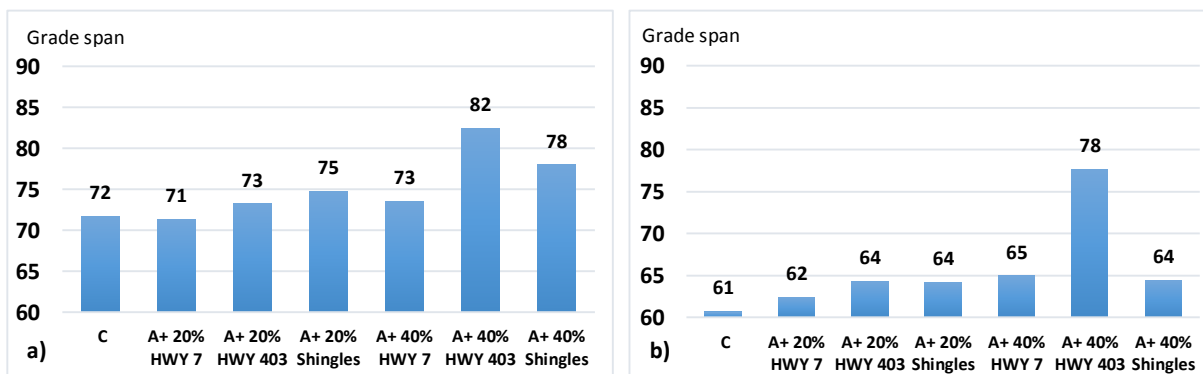


Figure 4.11: Grade span comparison of base C with A + RAP blends a) Unaged b) PAV-20 h aged samples.

There are no big differences of grade spans of A + 20 % RAP and RAS with base C. Even after adding 40 % recycled Hwy 7 into A, grade span difference is not significant with the base C (see Figure 4.12). This shows that the addition of 40 % recycle Hwy 7 into base A results in a relatively well performed binder as with base C.

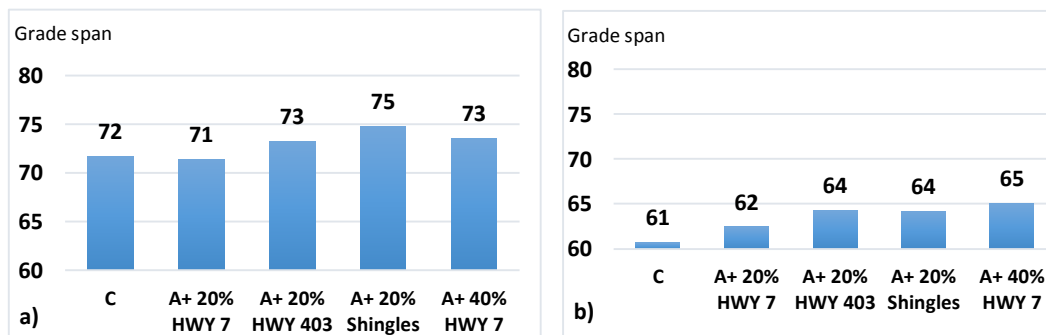


Figure 4.12: Grade span comparison of base C with A + RAP blends a) Unaged b) PAV-20 h aged samples.

#### 4.1.4 High Temperature Performance Grade with Limiting Phase Angle

Plotting the HTPG against limiting temperatures is one of the best methods to compare different binders. If different binders show similar properties, data points tend to distribute in a narrow range. To the better investigate of similarities between C and A based RAP blends, HTPG has been plotted against both  $T_{\delta=30^\circ}$  and  $T_{\delta=45^\circ}$  limiting temperatures at unaged and PAV-20 h aged conditions (see Figures 4.13 and 4.14).

<i>C</i>	<i>C</i>
<i>A+ 20% Hwy 7</i>	<i>D</i>
<i>A+ 20% Hwy 403</i>	<i>E</i>
<i>A+ 20% RAS</i>	<i>F</i>
<i>A+ 40% Hwy 7</i>	<i>G</i>

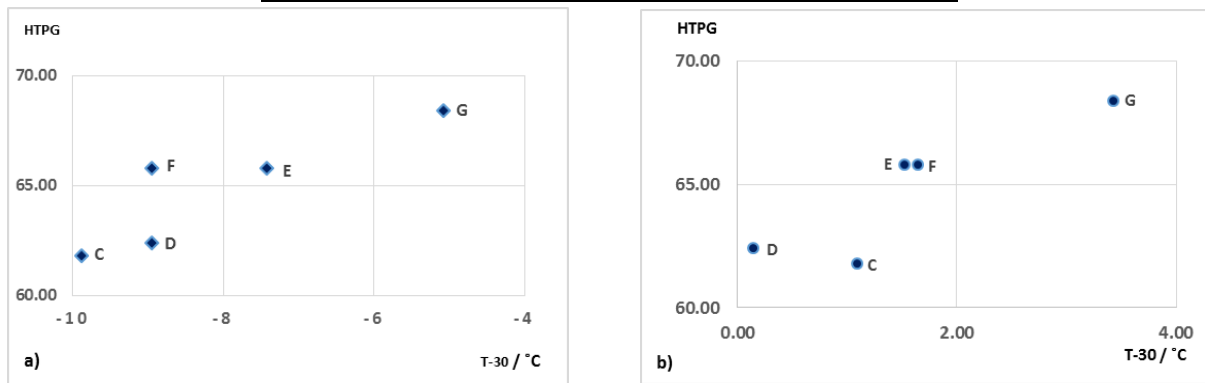


Figure 4.13: High temperatures performance grad vs. limiting temperature at phase angle 30° for C and A+ RAP. a) Unaged samples, b) PAV-20 h aged samples.

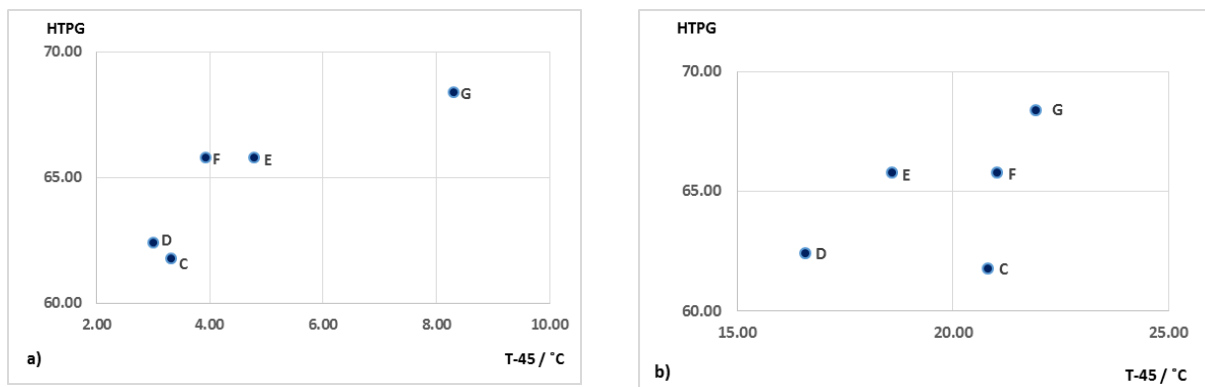


Figure 4.14: High temperatures performance grad vs. limiting temperature at phase angle 45° for C and A+ RAP. a) Unaged samples, b) PAV-20 h aged sample.

It can be seen that data point distribution is very narrow in each case. Both X-axis and Y-axis ranges are lower than 10. Specifically, data points for samples C, D, E and F show very narrow distribution and, G has deviated somewhat from those 4 points. This deviation should be due to the high RAP percentage in sample G. Hence, the addition of 20 % RAP to A makes a proper alternative to C. This simultaneous comparison of HTPG and limiting temperatures proves the ability of using A + RAP blends in place of C.

#### 4.1.5 Black Space Diagram

Black space diagrams are commonly used to compare different asphalt samples. If graphs are overlapping each other, this indicates that different samples show almost the same stiffness and stress relaxation abilities. Here Black space diagrams are plotted to provide further confirmation of performance similarities between C and A + RAP samples.

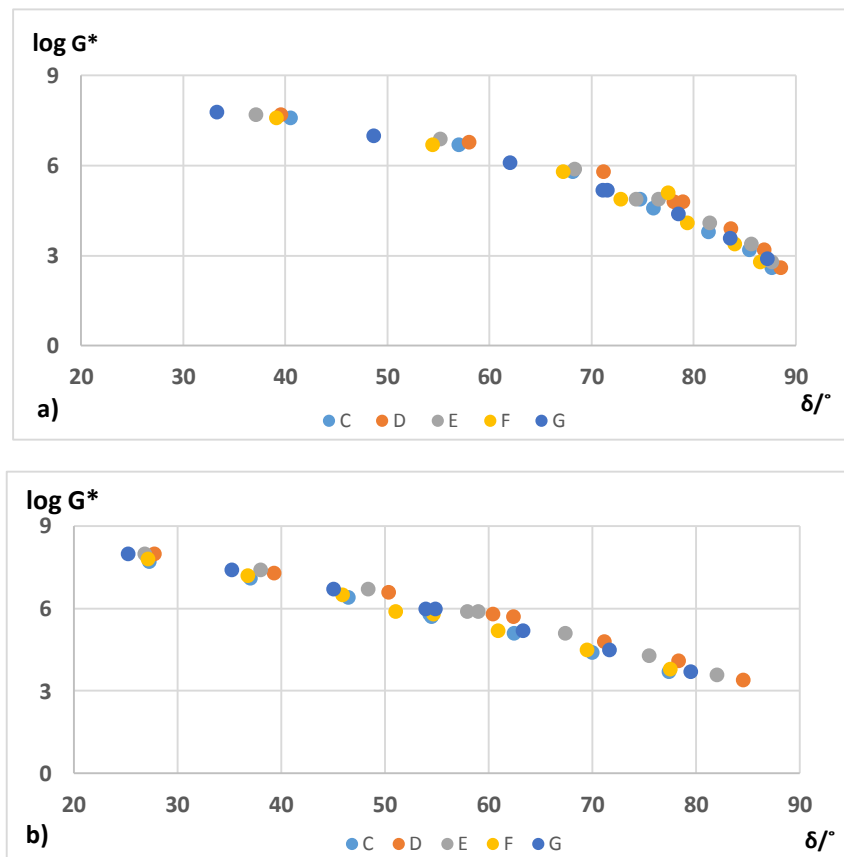


Figure 4.15: Black space diagrams for C and A+ RAP. a) Unaged samples, b) PAV-20 h aged samples.

According to figure 4.15, plots for all samples overlap in both unaged and PAV-20 hours aged conditions. Eventually, DSR results validated the ability to use A+RAP as an alternative to C.

#### 4.2 FTIR Analysis

FTIR data have been used to analyze oxidation level changes in base binders with the addition of RAP and with aging. The presence of carbonyl and sulfoxide is a good indication of the oxidation level in a particular binder. When the amount of carbonyl and sulfoxide is high in a binder, which indicates that the binder is highly oxidized. Binders become brittle and stiffer with the oxidation. The sulfoxide peak in aged asphalts generally have higher values compared to carbonyl peaks, which is associated with the high content of sulfur in the binder [76].

Table 4.2: Carbonyl Indices for Asphalt Blends (expressed in  $\times 10^3$ )

Sample ID	Aging condition			
	Unaged	RTFO	PAV-20	PAV-40
C	0.0	1.3	4.1	9.6
C+ 20% HWY 7	1.7	5.7	12.2	13.0
C+ 20% HWY 403	5.5	6.9	10.2	10.4
C+ 20% Shingles	2.7	2.8	8.1	10.5
C+ 40% HWY 7	7.3	8.3	10.3	12.2
C+ 40% HWY 403	11.5	10.8	15.8	17.4
C+ 40% Shingles	4.8	6.4	9.8	13.3
A	0.0	0.0	5.9	13.0
A+ 20% HWY 7	0.0	0.0	9.8	11.4
A+ 20% HWY 403	0.0	1.9	7.9	14.6
A+ 20% Shingles	0.0	1.3	9.9	17.1
A+ 40% HWY 7	3.3	5.6	12.7	11.9
A+ 40% HWY 403	5.9	13.6	12.3	14.1
A+ 40% Shingles	1.8	4.4	11.2	18.1

Table 4.3: Sulfoxide Indices for Asphalt Blends (expressed in  $\times 10^3$ )

Sample ID	Aging condition			
	Unaged	RTFO	PAV-20	PAV-40
C	3.2	10.0	13.5	15.5
C+ 20% HWY 7	9.5	14.7	26.3	26.2
C+ 20% HWY 403	11.3	11.7	19.4	18.5
C+ 20% Shingles	7.5	9.2	18.5	20.5
C+ 40% HWY 7	17.0	15.8	19.3	21.6

C+ 40% HWY 403	15.9	13.8	20.9	22.5
C+ 40% Shingles	8.3	9.5	17.0	18.9
A	5.4	9.7	13.9	13.5
A+ 20% HWY 7	10.0	14.1	22.5	19.1
A+ 20% HWY 403	9.9	12.2	16.1	21.6
A+ 20% Shingles	10.0	15.4	20.5	21.1
A+ 40% HWY 7	17.4	15.1	23.9	19.1
A+ 40% HWY 403	16.3	19.3	17.7	17.7
A+ 40% Shingles	9.2	11.2	16.7	21.7

It can be seen in table 4.2 and 4.3, the carbonyl and sulfoxide indexes increase with the aging and the addition of RAP and RAS. Both indexes in unaged binders C and A are lower than RAP and RAS added unaged blends. Also, both indexes are increasing with an increase in the RAP percentage. Overall, high index values appear in PAV-40 hours aging condition while low index values appear in the unaged conditions. This shows that oxidized material in the asphalt colloidal structure increase with time/aging. Besides, modified asphalt blends have relatively higher index values than base C and A as blends contain already aged RAP and RAS, and these have high contents of carbonyls and sulfoxides.

#### ***4.3 Hot Mixed Asphalt Test Results***

The Material Test Systems (MTS 810) servo-hydraulic test frame was used to conduct the Illinois Flexibility Index Tests (I-FIT) and Force-Displacement curves were plotted for each test (see Figure 4.16). The post peak slope ( $m$ ) was directly obtained from the curves, and normalized fracture energy ( $G_f$ ) was calculated using the total area of the plot. Then, those two parameters are used to calculate the Flexibility Index (FI), which predicts the resistance to fracture of an asphalt mixture. The parameters  $G_f$ ,  $m$ , FI and the shape of the Force-Displacement curve are used to evaluate the effect on stiffness, cracking propagation velocity and total resistant to fracture of the HMA upon changing the asphalt binder and modifying the asphalt with RAP and PET.

### 4.3.1 Force-Displacement Curves

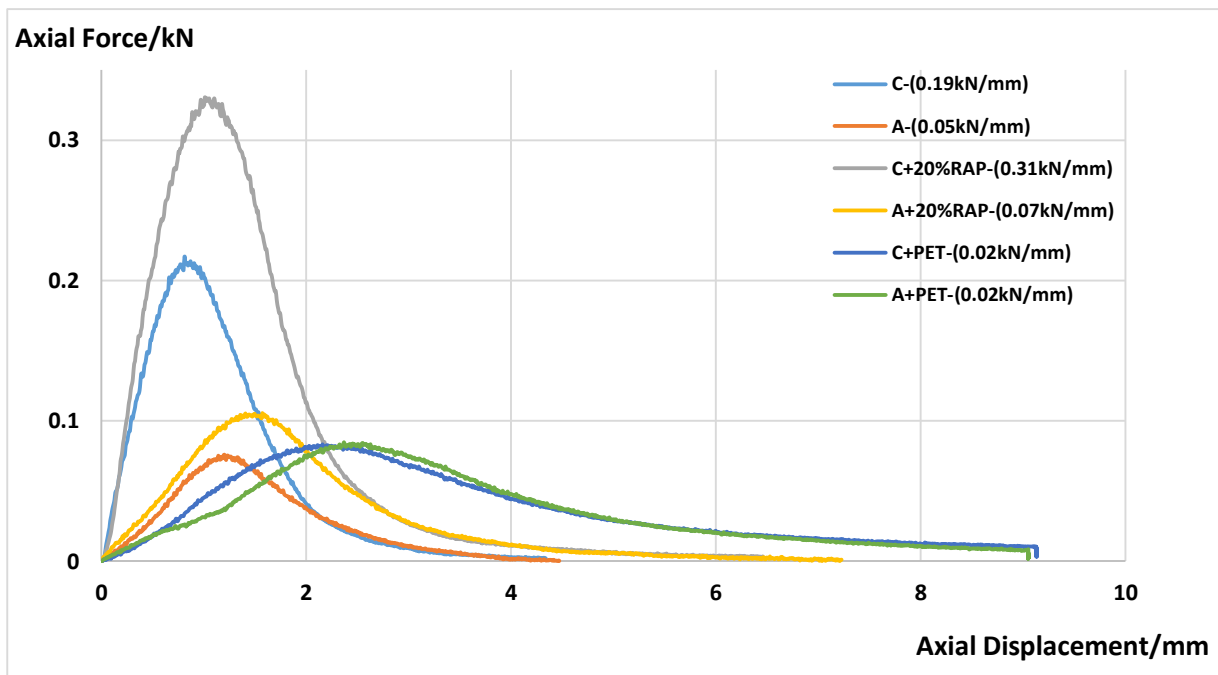


Figure 4.16: Force-Displacement curves at room temperature. (Post peak slopes are shown in the bracket after each series name).

The highest value for peak force appears in the C + 20% RAP specimen (over 0.3 kN) and the second-highest value for C (over 0.2 kN). The peak force for the other four specimens is below 0.1 kN. The trend is the same for post peak slope values ( $m$ ), where  $m$  for C+20 % RAP is 0.31 kN/mm and  $m$  for C is 0.19 kN/mm, and the value is below 0.1 kN/mm for the other four specimens. Usually, specimens with higher  $m$  values show high stiffness and high crack propagation velocity. The high crack propagation velocity may be due to the lower flexibility and the higher stiffness of the specimen. The flexibility of specimens can be evaluated by  $FI$  and the stiffness of specimen can be evaluated by  $G_f$ , which is discussed later in this chapter.

The addition of RAP into C significantly affects the  $m$  value where the value increases around 0.1 kN/mm. Hence, the C+20 % RAP specimen should be stiffer than C. On the other hand, the addition of PET into C drastically decreases the  $m$  value, and the difference is 0.17 kN/mm. It can be assumed that the flexibility of the specimen increases with the addition of PET. The  $m$  value for A is 0.05 kN/mm which increases up to 0.07 kN/mm with the addition

of 20 % RAP, such that the difference is not considerable. RAP in A may not significantly affect the stiffness and the flexibility of A. A + PET also shows a relatively similar  $m$  value as A. Also, the  $m$  value for both C + PET and A + PET are similar to each other (0.02 kN/mm).

Overall, the C specimen may initially be stiffer than A, and the addition of RAP and PET may significantly affect the stiffness and the flexibility of C. It seems that the properties of A do not change dramatically with the RAP addition and the A + 20 % RAP specimen may be more flexible than C. The flexibility and the stiffness may be almost similar in both C + PET and A + PET specimens.

#### ***4.3.2 Normalized Fracture Energy ( $G_f$ )***

One of the primary outputs of I-FIT is the normalized fracture energy,  $G_f$ , which represents the energy dissipated by the crack propagation [61]. The fracture energy is a function of both the strength and ductility of the material, which are related to the peak load and maximum displacement, respectively [61]. Peak load is increasing with the increase in the brittleness/stiffness of the sample. Generally, the higher the fracture energy, the better the cracking resistance. However, it has been observed that mixtures that exhibit the opposite behavior may present similar fracture energy values [77]. For instance, in the I-FIT, a brittle material, usually manifested by a high peak load and low ductility, may have a similar fracture energy to a material with high ductility and a lower peak load [77].

The brittleness/stiffness of the binder increases with decreasing temperature, which results in a high peak load value in the force displacement curve. Hence, the normalized fracture energy can be higher at lower temperatures than at room temperature for same type specimen (see Figure 4.17).

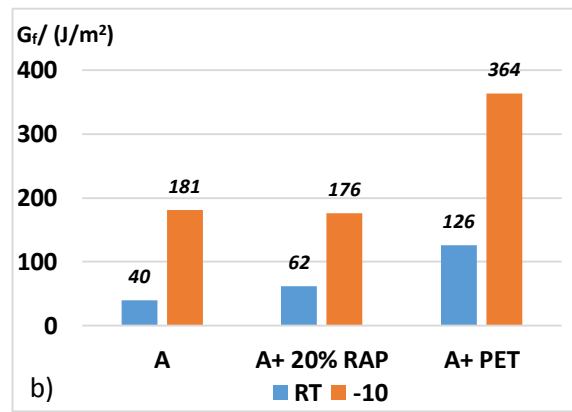
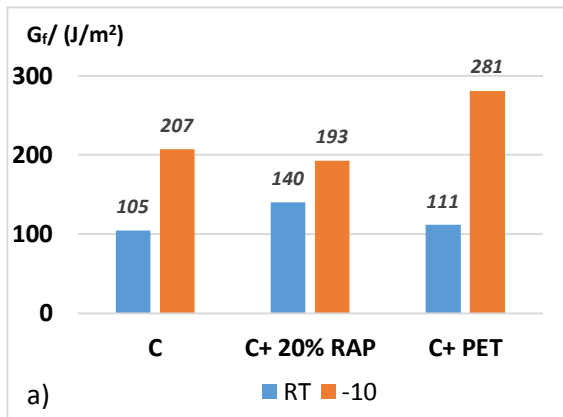


Figure 4.17: Normalized fracture energies at room temperature and -10 °C. a) C and modified C specimens, b) A and modified A specimens.

In both cases and all specimens,  $G_f$  is high at lower temperature (-10 °C), this must be due to the high stiffness of the asphalt binder at low temperatures.  $G_f$  of C and C+20 % RAP are higher than the  $G_f$  of A and A + 20 % RAP at both temperatures, and this may be due to the initial high stiffness of C. There is no significant difference in the  $G_f$  values in C + PET and A + PET. It is assumed that the addition of PET into the mixture drastically increases the ductility of the specimen.

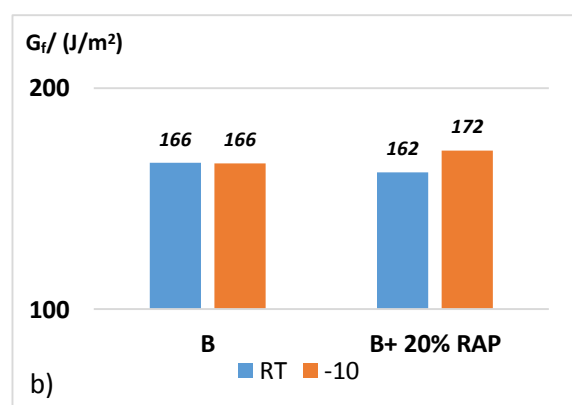
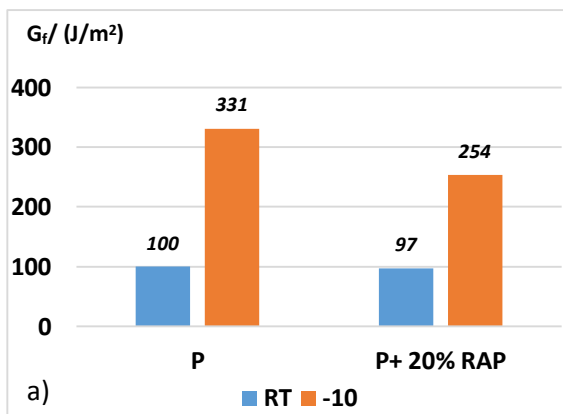


Figure 4.18: Normalized fracture energies at room temperature and -10 °C. a) P and modified P specimens, b) B and modified B specimens.

Temperature affects  $G_f$  in the mixture P and P + 20 % RAP, but the addition of RAP to P does not significantly effect the  $G_f$  of P. According to the graph b, both temperature and RAP do not have a considerable effect on  $G_f$  of mixture B.

### 4.3.3 Flexibility Index (FI)

FI has an excellent discrimination potential to analyze RAP and PET modified HMA. It is known that materials with relatively high FI show better cracking resistance than materials with relatively low FI. According to Ozer et al., an asphalt mixture provide excellent cracking resistance if it has a FI value over 10 and has a generally poor cracking resistance for a FI value below 6.

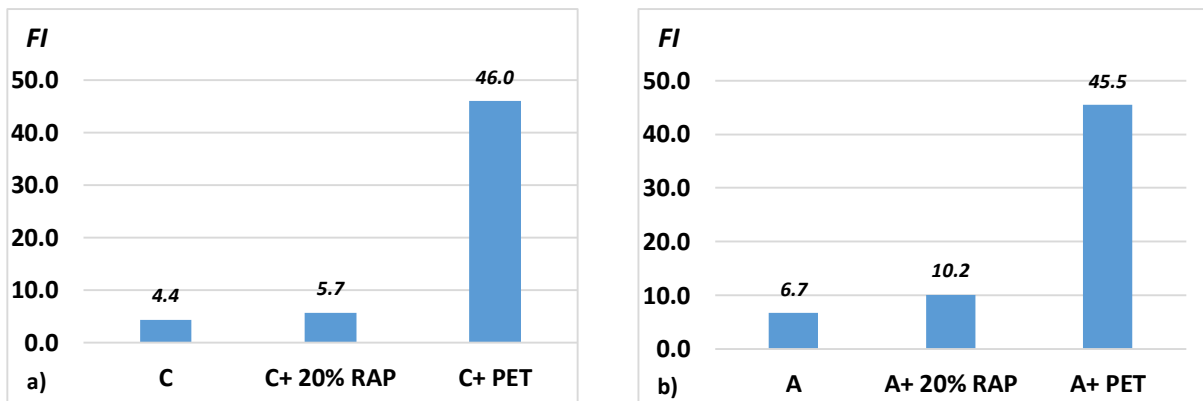


Figure 4.19: FI of HMA at room temperature. a) C and modified C mixtures, b) A and modified A mixtures.

The general trend for both samples is that FI slightly increases with the addition of RAP and drastically increases with the addition of PET (see Figure 4.19). It reveals that PET modified HMA has the highest cracking resistance and HMA with neat asphalt is relatively susceptible to premature cracking.

The FI value is slightly higher in C + 20 % RAP than C, with the difference being 1.3. This must be due to the small increase in  $G_f$  with the addition of RAP. It seems that there is no big effect on ductility of the C with adding 20% RAP. The C+PET mixture shows a high FI value, and is different from C, which is over 40. PET must improve the ductility of the HMA and it must show very high cracking resistance.

The FI of A increases with adding RAP and the different is about 3.5. This difference is considerable and this must be due to the  $G_f$  increment with the addition of RAP. The value for A+20% RAP is above 10, and this must show higher premature cracking resistance. The addition of PET into A is also results in a drastic increase in the FI value, where the FI value is over 45 for A + PET mixture.

The FI is initially higher in A than C, and this reveals that A should be more flexible and resistant to fatigue cracking than C. According to these two graphs, additions of PET into both C and A result in high flexibility and cracking resistance. Also, addition of RAP may increase the stiffness of the sample, but cracking resistance should be higher with RAP. According to these results, the use of 20 % RAP with base asphalt binder is advisable. Specially, addition of RAP into A gives favorable results.

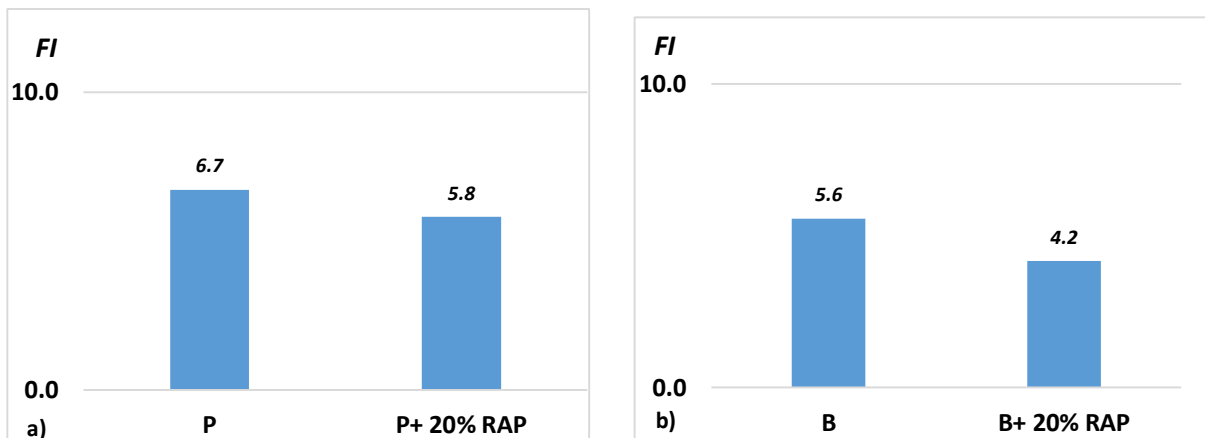


*Figure 4.20: FI of HMA at room temperature. a) P and modified P mixtures, b) B and modified B mixtures.*

All four mixtures have relatively similar FI values. In the both cases, FI is slightly lower with the addition of RAP (see Figure 4.20). It must be due to the ductility decrement after the RAP addition. However, the effect on FI with RAP is not considerable for both P and B. P is initially more flexible than B and also, P + 20 % RAP has almost same flexibility as B. It seems

that P + 20% RAP shows equal cracking resistance properties as B. When consider on FI, P + 20 % RAP can be used as an alternative to B.

## *Chapter 5*

### *Summary and Conclusions*

The HTPG difference between A and C shows that the A is softer than C, where C has higher rutting resistance than A and, A should have a higher resistance to fatigue and thermal cracking. The addition of RAP and RAS into base asphalt and aging of asphalt binder result in high HTPG, which shows that the brittleness of asphalt binders increase with RAP modifications and aging. Hence, RAP modifications and aging ended up with very high rutting resistance and low fatigue and thermal resistance.

Because of the initial high stiffness of C, RAP and RAS modified C base binders have higher HTPG than A based blends. There should be more asphaltene content in C based blends than in A based blends. Therefore, the colloidal stability of C based blends should be lower than the colloidal stability of A based blends. This reveals that softer A base asphalt can accommodate more RAP percentage than C base asphalt,

Both limiting temperatures ( $T_{\delta=30^\circ}$  and  $T_{\delta=45^\circ}$ ) are higher in C than A in both unaged and PAV-20 h of aging conditions, which shows that A can relax the stress more efficiently than C. Limiting temperatures increase with the aging and RAP modifications. It can be observed that brittle binders have higher limiting temperatures than soft asphalt. Also, results show that limiting temperatures of C based blends are higher than the corresponding A based blends.

The grade span is higher in C than A in both unaged and PAV-20 h aging conditions. Also, the grade span for C-based asphalt blends is higher than the grade span of A based blends. These results also reveal the comparatively high stiffness of the C.

The overall analysis of HTPG, limiting temperatures and grade span exhibit that A + 20 % RAP blends perform similarly to the well performing C base binder. HTPG vs limiting temperature graphs show that data points for C, D, E, F and G samples are in a narrow range.

Besides, black space diagrams for C, D, E, F and G almost overlap each other. Hence, DSR results prove that A + 20 % RAP can be used as an alternative for the C binder.

According to I-FIT results, A is more flexible than C and the addition of 20 % RAP into both C and A increases the  $G_f$  and FI of binders. The addition of PET into both C and A results in a drastic increment of FI and the FI values difference between PET-modified A and C is not significant. This shows that the ductility of the HMA is significantly increased by PET in both C and A HMA.

## References

1. Valdes-Vidal, G., Calabi-Floody, A., & Sanchez-Alonso, E. (2018). Performance evaluation of warm mix asphalt involving natural zeolite and reclaimed asphalt pavement (RAP) for sustainable pavement construction. *Construction and Building Materials*, 174, 576-585.
2. Copeland, A. (2011). Reclaimed asphalt pavement in asphalt mixtures: State of the practice (No. FHWA-HRT-11-021). United States. Federal Highway Administration. Office of Research, Development, and Technology.
3. Ding, H., Gyasi, J., Hesp, S. A., Marks, P., Nie, Y., Somuah, M., & Ubaid, I. (2018). Performance grading of extracted and recovered asphalt cements. *Construction and Building Materials*, 187, 996-1003.
4. Behnia, B., Dave, E. V., Ahmed, S., Buttlar, W. G., & Reis, H. (2011). Effects of recycled asphalt pavement amounts on low-temperature cracking performance of asphalt mixtures using acoustic emissions. *Transportation Research Record*, 2208(1), 64-71.
5. R. Schreck, More RAP in HMA: Is it worth it? The 2007 Virginia RAP initiative, *HMAT: Hot Mix Asphalt Technol.* 12 (4) (2007) 10–13.
6. Yang, R., Kang, S., Ozer, H., & Al-Qadi, I. L. (2015). Environmental and economic analyses of recycled asphalt concrete mixtures based on material production and potential performance. *Resources, Conservation and Recycling*, 104, 141-151.
7. El-Korchi, T., & Mallick, R. B. (2007). Accelerated testing methodology for evaluating pavement patching materials (No. 07-3021).
8. Tetteh, N. (2018). Rheological evaluation of field-aged asphalt cements (Masters' dissertation, Queen's University (Canada)).
9. Asphalt Institute (Ed.). (2003). Performance graded asphalt binder specification and testing (No. 1). Asphalt Institute.
10. Lesueur, D. (2009). The colloidal structure of bitumen: Consequences on the rheology and on the mechanisms of bitumen modification. *Advances in colloid and interface science*, 145(1-2), 42-82.
11. Arias, G. K. B. (2019). Influence of Oxidative Aging on the Chemistry and Rheology of Asphalt Cement from Bolivian, Canadian and Costa Rican Sources (Doctoral dissertation, Queen's University (Canada)).
12. R. Hunter, D. Whiteoak, J. Read, *The Shell Bitumen Handbook*, 5th Ed., Thomas Telford Publishing, (2003).
13. Hein, F. J. (2006). Heavy oil and oil (tar) sands in North America: an overview & summary of contributions. *Natural Resources Research*, 15(2), 67-84.
14. Meyer, R. F., Attanasi, E. D., & Freeman, P. A. (2007). Heavy oil and natural bitumen resources in geological basins of the world: Map showing klemme basin classification of sedimentary provinces reporting heavy oil or natural bitumen. *US Geol. Surv. Open-File Rep*, 2007, 1084.
15. Sirin, O., Paul, D. K., & Kassem, E. (2018). State of the art study on aging of asphalt mixtures and use of antioxidant additives. *Advances in Civil Engineering*, 2018.
16. Abbas, A. R., Nazzal, M., Kaya, S., Akinbowale, S., Subedi, B., Arefin, M. S., & Abu Qtaish, L. (2016). Effect of aging on foamed warm mix asphalt produced by water injection. *Journal of Materials in Civil Engineering*, 28(11), 04016128.

17. <https://pavementinteractive.org/reference-desk/testing/binder-tests/rolling-thin-film-oven>, 27/05/2020, 5.30 PM.
18. <https://www.humboldtmg.com/asphalt-rolling-thin-film-oven.html>, 27/05/2020, 5.35 PM.
19. <https://pavementinteractive.org/reference-desk/testing/binder-tests/pressure-aging-vessel/>, 27/05/2020, 5.40 PM.
20. Ghanoun, S. A., & Tanzadeh, J. (2019). Laboratory evaluation of nano-silica modification on rutting resistance of asphalt Binder. *Construction and Building Materials*, 223, 1074-1082.
21. Du, Y., Chen, J., Han, Z., & Liu, W. (2018). A review on solutions for improving rutting resistance of asphalt pavement and test methods. *Construction and Building Materials*, 168, 893-905.
22. Zou, G., Xu, J., & Wu, C. (2017). Evaluation of factors that affect rutting resistance of asphalt mixes by orthogonal experiment design. *International Journal of Pavement Research and Technology*, 10(3), 282-288.
23. <https://everythingroads.com/2018/know-thy-enemy-rutting>, 29/05/2020, 1.30 PM
24. Cooper, K. E., and P. S. Pell. The Effect of Mix Variables on the Fatigue Strength of Bituminous Materials. Report LR633. United Kingdom Transport and Road Research Laboratory, Crowthorne, Berkshire, England, 1974.
25. Andriescu, A., Gibson, N., Hesp, S., Qi, X., & Youtcheff, J. (2006). Validation of the essential work of fracture approach to fatigue grading of asphalt binders. *ASPHALT PAVING TECHNOLOGY*, 75, CD1.
26. <https://www.researchgate.net/figure/Fatigue-cracking-encountered-on-pavement>, 29/05/2020, 1.35 PM.
27. Isacson, U., & Zeng, H. (1997). Relationships between bitumen chemistry and low temperature behaviour of asphalt. *Construction and Building Materials*, 11(2), 83-91.
28. Voigt, G.F. Early cracking of concrete pavement-causes and repairs. in 2002 Federal Aviation Administration (FAA) Airport Technology Transfer Conference. 2002. Citeseer.
29. <https://www.pwri.go.jp/eng/about/pr/webmag/wm022/seika.html>, 29/05/2020, 1.40 PM
30. Zhang, J., Airey, G. D., Grenfell, J., & Apeageyi, A. K. (2018). Moisture sensitivity examination of asphalt mixtures using thermodynamic, direct adhesion peel and compacted mixture mechanical tests. *Road Materials and Pavement Design*, 19(1), 120-138.
31. Somuah, M. (2016). Investigative Comparison of Tank and Recovered Asphalt Samples Through Physical Performance Testing and Chemical Analysis (Masters' dissertation).
32. <http://www.asphaltinstitute.org/laboratory/testing-services/individual-asphalt-binder-tests>, 25/05/2020 at 1.45 PM
33. <https://wecivilengineers.wordpress.com/2018/01/22/penetration-test-of-bitumen>, 25/05/2020, 1.50 PM
34. Gyasi, J. (2018). Comparative study of the effects of physical and chemical aging on extracted and recovered asphalt binders from some municipal and provincial roads in Canada (Masters' dissertation, Queen's University (Canada)).

35. <https://theconstructor.org/practical-guide/ring-ball-softening-point-bitumen-asphalt-tar>, 25/05/2020, 2.00 PM
36. Li, R., Wang, C., Wang, P., & Pei, J. (2016). Preparation of a novel flow improver and its viscosity-reducing effect on bitumen. *Fuel*, 181, 935-941.
37. <https://pavementinteractive.org/reference-desk/materials/asphalt/viscosity-grading>, 25/05/2020 at 1.47 PM
38. <https://www.coleparmer.ca/p/brookfield-rotational-viscometers/22463>, 25/05/2020, 7.00 PM
39. <https://www.directindustry.com/prod/cannon-instrument-company/product-106453-2074879.html>, 25/05/2020, 7.04 PM
40. <https://pavementinteractive.org/reference-desk/design/mix-design/superpave-overview>, 25/05/2020, 8.00 PM
41. Marsac, P., Piérard, N., Porot, L., Grenfell, J., Mouillet, V., Pouget, S., & Hugener, M. (2014). Potential and limits of FTIR methods for reclaimed asphalt characterisation. *Materials and structures*, 47(8), 1273-1286.
42. Hofko, B., Porot, L., Cannone, A. F., Poulikakos, L., Huber, L., Lu, X., & Grothe, H. (2018). FTIR spectral analysis of bituminous binders: reproducibility and impact of ageing temperature. *Materials and Structures*, 51(2), 45.
43. Weigel, S., & Stephan, D. (2017). The prediction of bitumen properties based on FTIR and multivariate analysis methods. *Fuel*, 208, 655-661.
44. <https://www.ssi.shimadzu.com/products/ftir-spectrophotometers/iraffinity-1s.html>, 09/11/2020, 3.00 PM
45. Carret, J. C., Falchetto, A. C., Marasteanu, M. O., Di Benedetto, H., Wistuba, M. P., & Sauzeat, C. (2015). Comparison of rheological parameters of asphalt binders obtained from bending beam rheometer and dynamic shear rheometer at low temperatures. *Road Materials and Pavement Design*, 16(sup1), 211-227.
46. <https://pubs.rsc.org/en/content/chapterhtml/2019/bk9781788013963-00001?isbn=978-1-78801-396-3&sercode=bk>, 26/05/2020 at 6.00 PM
47. <https://wiki.anton-paar.com/en/basics-of-rheology>, 26/05/2020 at 6.15 PM
48. <https://wiki.anton-paar.com/en/basics-of-rheology>, 26/05/2020 at 6.15 PM
49. <https://www.slideshare.net/hronaldo10/04superpave-binder-testing-highway-and-airport-engineering-dr-sherif-elbadawy>, 26/05/2020 at 10.24 PM
50. <https://www.tainstruments.com/dhr-1>, 26/05/2020 at 10.47 PM
51. Hesp, S. A., & Subramani, S. (2009, July). Another look at the bending beam rheometer for specification grading of asphalt cements. In *Proceedings of 6th MAIREPAV Conference*, Torino, Italy.
52. [https://www.researchgate.net/figure/Bending-Beam-Rheometer\\_fig1\\_306201785](https://www.researchgate.net/figure/Bending-Beam-Rheometer_fig1_306201785), 29/05/2020 at 12.42 AM
53. [http://www.studiocesaingegneria.it/SUPERPAVE/Test%20BBR%20\(7\)/Test%20BBR.htm](http://www.studiocesaingegneria.it/SUPERPAVE/Test%20BBR%20(7)/Test%20BBR.htm), 29/05/2020 at 12.48 AM
54. Hesp, S. A., Soleimani, A., Subramani, S., Phillips, T., Smith, D., Marks, P., & Tam, K. K. (2009). Asphalt pavement cracking: analysis of extraordinary life cycle variability in eastern and northeastern Ontario. *International Journal of Pavement Engineering*, 10(3), 209-227.

55. Paliukaitė, M., Assuras, M., Silva, S. C., Ding, H., Gotame, Y., Nie, Y., & Hesp, S. A. (2017). Implementation of the double-edge-notched tension test for asphalt cement acceptance. *Transportation in Developing Economies*, 3(1), 6.
56. Asiedu, E. Investigating and Understanding the Effects of Reclaimed Asphalt Pavement and Shingles on the Rheology and Performance Grading of Asphalt Cement (Masters' dissertation).
57. [https://www.researchgate.net/figure/a-Schematic-of-double-edge-notched-tension-specimen-design-and-b-picture-of-sample\\_fig1\\_245561065](https://www.researchgate.net/figure/a-Schematic-of-double-edge-notched-tension-specimen-design-and-b-picture-of-sample_fig1_245561065), 30/05/2020 at 12.03 AM
58. [https://www.researchgate.net/figure/Double-edge-notched-tension-test-specimens-with-5-10-and-15-mm-ligaments-just-prior-to\\_fig1\\_283459976](https://www.researchgate.net/figure/Double-edge-notched-tension-test-specimens-with-5-10-and-15-mm-ligaments-just-prior-to_fig1_283459976), 30/05/2020 at 12.06 AM
59. Asphalt Institute. (2014). MS-2 asphalt mix design methods. Asphalt Institute.
60. <https://www.pinetestequipment.com/product/g2-gyratory-compactor>, 09/11/2020, 5.30 PM
61. Batioja-Alvarez, D., Lee, J., & Haddock, J. E. (2019). Understanding the Illinois Flexibility Index Test (I-FIT) using Indiana Asphalt Mixtures. *Transportation Research Record*, 2673(6), 337-346.
62. Ozer, H., Al-Qadi, I. L., Lambros, J., El-Khatib, A., Singhvi, P., & Doll, B. (2016). Development of the fracture-based flexibility index for asphalt concrete cracking potential using modified semi-circle bending test parameters. *Construction and Building Materials*, 115, 390-401.
63. Selvavathi, V., Sekar, V. A., Sriram, V., & Sairam, B. (2002). Modifications of bitumen by elastomer and reactive polymer comparative study. *Petroleum science and technology*, 20(5-6), 535-547.
64. Paliukaite, M., Assuras, M., & Hesp, S. A. (2016). Effect of recycled engine oil bottoms on the ductile failure properties of straight and polymer-modified asphalt cements. *Construction and Building Materials*, 126, 190-196.
65. Ahmad, A. F., Razali, A. R., & Razelan, I. S. M. (2017, April). Utilization of polyethylene terephthalate (PET) in asphalt pavement: A review. In *Proceedings of the Mechanical Engineering, Science and Technology International Conference*.
66. Movilla-Quesada, D., Raposeiras, A. C., & Olavarría, J. (2019). Effects of Recycled Polyethylene Terephthalate (PET) on Stiffness of Hot Asphalt Mixtures. *Advances in Civil Engineering*, 2019.
67. Ji, J., Yao, H., Suo, Z., You, Z., Li, H., Xu, S., & Sun, L. (2017). Effectiveness of vegetable oils as rejuvenators for aged asphalt binders. *Journal of Materials in Civil Engineering*, 29(3), D4016003.
68. Zaumanis, M., Mallick, R. B., & Frank, R. (2014). 100% recycled hot mix asphalt: A review and analysis. *Resources, Conservation and Recycling*, 92, 230-245.
69. Hussain, A., & Yanjun, Q. (2013). Effect of reclaimed asphalt pavement on the properties of asphalt binders. *Procedia Engineering*, 54, 840-850.
70. Garcia Cucalon, L., Kaseer, F., Arámbula-Mercado, E., Epps Martin, A., Morian, N., Pournoman, S., & Hajj, E. (2019). The crossover temperature: significance and application towards engineering balanced recycled binder blends. *Road Materials and Pavement Design*, 20(6), 1391-1412.
71. 49. Singh, D., & Sawant, D. (2016). Understanding effects of RAP on rheological performance and chemical composition of SBS modified binder using series of

- laboratory tests. *International Journal of Pavement Research and Technology*, 9(3), 178-189.
72. Zhang, J., Sun, H., Jiang, H., Xu, X., Liang, M., Hou, Y., & Yao, Z. (2019). Experimental assessment of reclaimed bitumen and RAP asphalt mixtures incorporating a developed rejuvenator. *Construction and Building Materials*, 215, 660-669.
73. Oyekunle, L. O. (2006). Certain relationships between chemical composition and properties of petroleum asphalts from different origin. *Oil & Gas Science and Technology-Revue de l'IFP*, 61(3), 433-441.
74. Garcia Cucalon, L., King, G., Kaseer, F., Arambula-Mercado, E., Epps Martin, A., Turner, T. F., & Glover, C. J. (2017). Compatibility of recycled binder blends with recycling agents: rheological and physicochemical evaluation of rejuvenation and aging processes. *Industrial & Engineering Chemistry Research*, 56(29), 8375-8384.
75. <https://www.globalgilson.com/ats-rolling-thin-film-oven>, 12/12/2020, 1.30 PM
76. Martin, K. L., Davison, R. R., Glover, C. J., & Bullin, J. A. (1990). Asphalt aging in Texas roads and test sections. *Transportation Research Record*, (1269).
77. Kaseer, F., Yin, F., Arámbula-Mercado, E., Martin, A. E., Daniel, J. S., & Salari, S. (2018). Development of an index to evaluate the cracking potential of asphalt mixtures using the semi-circular bending test. *Construction and Building Materials*, 167, 286-298.